

Safeguarding Data in Multimodal AI: A Differentially Private Approach to CLIP Training

Alyssa Huang^{*||} Peihan Liu^{†||} Ryumei Nakada^{‡||} Linjun Zhang^{§**}
Wanrong Zhang^{¶**}

Abstract

The surge in multimodal AI’s success has sparked concerns over data privacy in vision-and-language tasks. While CLIP has revolutionized multimodal learning through joint training on images and text, its potential to unintentionally disclose sensitive information necessitates the integration of privacy-preserving mechanisms. We introduce a differentially private adaptation of the Contrastive Language-Image Pretraining (CLIP) model that effectively addresses privacy concerns while retaining accuracy. Our proposed method, DP-CLIP, is rigorously evaluated on benchmark datasets encompassing diverse vision-and-language tasks such as image classification and visual question answering. We demonstrate that our approach retains performance on par with the standard non-private CLIP model. Furthermore, we analyze our proposed algorithm under linear representation settings. We derive the convergence rate of our algorithm and show a trade-off between utility and privacy when gradients are clipped per-*batch* and the loss function does not satisfy smoothness conditions assumed in the literature for the analysis of DP-SGD.

1 Introduction

The field of vision-language tasks has witnessed a revolutionary breakthrough with the introduction of Contrastive Language-Image Pre-training (CLIP) (Radford et al., 2021) by OpenAI. It has redefined the benchmarks of various downstream vision-language tasks through its exceptional flexibility and remarkable zero-shot learning ability (Li et al., 2021b; Dorbala et al., 2022). CLIP and its successors have been widely used in vision-language tasks such as semantic segmentation, image generation from captions, video summarization, and visual question answering (Galatolo et al., 2021; Narasimhan et al., 2021; Yao et al., 2021; Li et al., 2021c; Xu et al., 2022; Wang et al., 2022).

However, representations from contrastive learning are rich in information, which might be able to unintentionally memorize more personal sensitive information. Carlini et al. (2023) shows that diffusion models, which are built upon CLIP, can memorize individual images in the training data and emit them at generation time, and is even less private compared to prior generative models such as GANs. Liu et al. (2021) successfully conducts membership inference attacks on the image encoder trained from CLIP. Furthermore, He and Zhang (2021) demonstrates that SimCLR, another framework that employs contrastive learning for image representations, is more susceptible to attribute inference attacks compared to standard supervised models.

^{*}Harvard College. alyssahuang@college.harvard.edu.

[†]Harvard John A. Paulson School of Engineering and Applied Sciences. peihanliu@fas.harvard.edu.

[‡]Department of Statistics, Rutgers University. rn375@rutgers.edu.

[§]Department of Statistics, Rutgers University. linjun.zhang@rutgers.edu. Supported by NSF DMS-2015378.

[¶]Harvard John A. Paulson School of Engineering and Applied Sciences. wanrongzhang@fas.harvard.edu. Supported by a Computing Innovation Fellowship from the Computing Research Association (CRA) and the Computing Community Consortium (CCC).

^{||}Indicates equal contribution as first author.

^{**}Corresponding authors.

Mitigating these privacy vulnerabilities requires privacy-preserving training methods for multimodal models. The field of *Differential privacy* (DP) has emerged as the gold standard for privacy-preserving data analytics. It is a mathematical notion of privacy, which ensures that the output distribution of computation is robust to one person’s data. DP is typically achieved by introducing randomness in the computation. Differential privacy techniques have been employed in the context of unimodal models (Peng Xu, 2022; Basu et al., 2021; Hoory et al., 2021; Yu et al., 2022; Li et al., 2022b)

However, differentially private training of multimodal models is currently understudied. (Carlini et al., 2023) shows directly applying DP-SGD (Abadi et al., 2016) to diffusion models on CIFAR-10 causes the training consistently diverge, even when low privacy guarantees.

In this paper, we propose DP-CLIP, which safeguards vision-language tasks by learning differentially private image and text representations. These representations can then be safely used for various downstream multimodal tasks. We hope that, by leveraging the information contained in the pretrained embeddings using public data, our fine-tuned private representations can maintain their utility in performing various downstream tasks. Since the CLIP loss function involves contrasting data from different pairs, the standard DP deep learning approach, DP-SGD based on *per-sample* clipping based, cannot be directly applied. To address this challenge, we propose to use *per-batch* clipping and show that our algorithm achieves high accuracy while protecting the desired level of privacy, from both theoretical and empirical perspectives.

To demonstrate the strength of our proposed method, we evaluate our differentially private CLIP, DP-CLIP, on benchmark datasets encompassing diverse vision-and-language tasks such as image classification and visual question answering (VQA). The findings demonstrate that our privacy-aware approach retains performance on par with the standard CLIP model while significantly reducing the risk of data exposure. It is worth emphasizing that our work represents one of the first attempts to incorporate differential privacy into multimodal models, thus paving the way for enhanced privacy protection in vision-language tasks.

Furthermore, we theoretically derive the privacy-utility trade-off of DP-CLIP under linear representation settings with linearized loss. Previous works analyzed the convergence rate of DP-SGD under certain smoothness conditions (Yu et al., 2019; Bassily et al., 2019; Feldman et al., 2020; Chen et al., 2020a; Yang et al., 2022; Bu et al., 2022; Fang et al., 2023). However, we note that the CLIP loss function is not convex nor satisfy smoothness conditions in these literature. We also note that we deal with per-batch clipping instead of per-sample clipping analyzed in Abadi et al. (2016); Chen et al. (2020a); Yang et al. (2022); Bu et al. (2022); Fang et al. (2023). Although the loss function does not globally behave well, we exploit the fact that the linearized loss is locally smooth and strongly convex, and provide a probabilistic bound with linear convergence in the number of iterations.

The rest of this paper is organized as follows. We provide the necessary background for interpreting our results in Section 2. In Section 3, we introduce our algorithm DP-CLIP. We present our experiments setup and empirical results in Section 4, followed by our theoretical analysis in Section 5. Finally, we conclude with our discussion in Section 6.

2 Preliminaries

Differential Privacy *Differential Privacy* is a mathematical definition of privacy. It is used to enable the analysis of sensitive data while preserving the privacy of individuals, because of its powerful worst-case guarantees. In essence, differential privacy requires a mechanism’s outputs on two adjacent datasets, which differ in one arbitrary person’s data, should be indistinguishable. This is achieved by introducing randomness into the computation.

Definition 1 (Differential Privacy (Dwork et al., 2006)). *A randomized algorithm $M : \mathcal{X} \rightarrow \mathcal{Y}$ preserves (ϵ, δ) -differential privacy, if for all adjacent $X, X' \in \mathcal{X}$ s.t. $\forall S \subseteq \mathcal{Y}$,*

$$\Pr[M(X) \in S] \leq e^\epsilon \Pr[M(X') \in S] + \delta. \quad (2.1)$$

Differentially private mechanisms typically add noise that scales with the *sensitivity* of the function being evaluated. The sensitivity of a function f is defined as the maximum change in f between two neighboring sets:

$\Delta f = \max_{X, X' \text{ neighbors}} |f(X) - f(X')|$. The *Gaussian mechanism* with parameters (ϵ, δ) takes in a function q , dataset X , and outputs $f(X) + \mathcal{N}(0, \sigma^2)$, where $\sigma = \sqrt{2 \log(1.25/\delta)} \Delta f / \epsilon$. This canonical mechanism serves as a base for DP-SGD, which is the current state-of-the-art framework for DP deep learning.

Existing works have explored the effects of clipping and noise addition on the convergence and performance of DP deep learning models. Bu et al. (2021) analyzed the impact of per-sample clipping and noise addition on the convergence of DP deep learning models, characterizing these effects through training dynamics and the neural tangent kernel. They also introduced a new technique called *global clipping* that improves the convergence rate of DP-SGD. Wang et al. (2019) studied the convergence properties of DP-SGD and showed that it converges to an approximate local minimum with high probability. Imtiaz and Sarwate (2017) conducted differentially private canonical correlation analysis (DP-CCA) experiments to evaluate the effectiveness of differential privacy in preventing membership inference attacks. Yu et al. (2019) showed that gradient perturbation is efficient and accurate when the sample size is large and suggested that gradient perturbation may be combined with other differential privacy techniques to achieve even better results.

CLIP The *Contrastive Language-Image Pre-training* (CLIP) (Radford et al., 2021) is a multimodal vision and language model, trained on a variety of image and text pairs. It is used to produce embeddings for both texts and images. Specifically, let $f : \mathbb{R}^{d_1} \rightarrow \mathbb{R}^r$ and $\tilde{f} : \mathbb{R}^{d_2} \rightarrow \mathbb{R}^r$ be the dual encoders. Given pairs of data $\{(x_i, \tilde{x}_i)\}_{i \in [n]} \subset \mathbb{R}^{d_1+d_2}$, the CLIP loss can be formulated as follows:

$$\mathcal{L}(f, \tilde{f}) := -\frac{1}{n} \sum_{i \in [n]} \log \frac{e^{s_{ii}/\tau}}{\sum_{j \in [n]} e^{s_{ij}/\tau}} - \frac{1}{n} \sum_{i \in [n]} \log \frac{e^{s_{ii}/\tau}}{\sum_{j \in [n]} e^{s_{ji}/\tau}}, \quad (2.2)$$

where $s_{ij} := \text{Sim}(f(x_i), \tilde{f}(\tilde{x}_j))$ is the cosine similarity of x_i and \tilde{x}_j measured in the feature space, and $\tau > 0$ is the temperature parameter. The loss in equation 2.2 is a type of *contrastive loss*, that trains encoders by classifying based on whether a pair is observed or artificially paired. Intuitively, the loss 2.2 maps images and texts, that refer to the same object, to vectors with high cosine similarity and map images and texts that are unrelated to vectors with low cosine similarity. We provide the details of the pretraining process illustrated in 1.

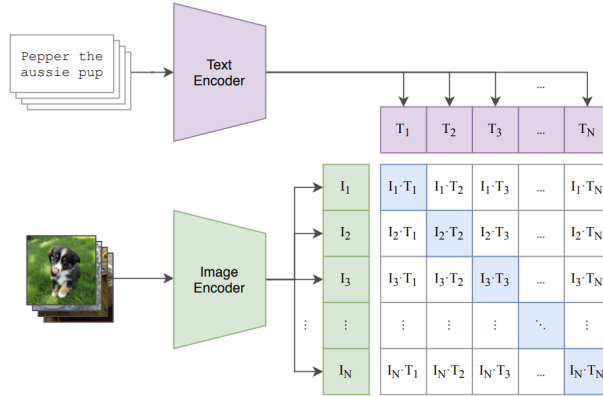


Figure 1: CLIP Pretraining Process From Radford et al. (2021)

3 DP-CLIP: Private and Accurate Representations

In this section, we introduce our DP-CLIP that incorporates differential privacy into the CLIP model, presented formally in Algorithm 1. Given initial representation functions, the algorithm trains encoders based

on per-batch noisy SGD to ensure privacy. The CLIP loss (Radford et al., 2021) is the contrastive cross-entropy loss function computed from pseudo-labels distinguishing whether a pair is observed or artificially generated. Since the CLIP loss function, by definition, contains the similarity between data from multiple pairs, it cannot be written as a sum of losses of individual pairs. Thus we cannot directly apply per-sample clipping technique as in the original DP-SGD. Instead, we employ *per-batch* clipping, and we show that can still guarantee the desired level of privacy, which we discuss in details below.

More specifically, we consider the following setups. Let f_{θ_1} and \tilde{f}_{θ_2} be the dual encoders to be trained, parameterized by θ_1 and θ_2 , respectively. Let $\theta^{(t)} = (\theta_1^{(t)}, \theta_2^{(t)})$ be the parameters at t -th iteration. We obtain a sequence of parameters $(\theta^{(t)})_{t=1}^T$ through mini-batch stochastic gradient descent, where T is the number of iterations. For any subset $\mathcal{B} \subset [n]$, define $\mathcal{L}(\cdot; \mathcal{B})$ be the loss 2.2 computed only with pairs $\{(x_i, \tilde{x}_i)\}_{i \in \mathcal{B}}$. At iteration t , we uniformly sub-sample a mini-batch $\mathcal{B}^{(t)}$ of size b from $[n]$ and compute the partial derivative of $\mathcal{L}(f_{\theta_1}, \tilde{f}_{\theta_2}; \mathcal{B}^{(t)})$, the loss computed with mini-batch, with respect to θ evaluated at $\theta_1 = \theta_1^{(t)}$ and $\theta_2 = \theta_2^{(t)}$. We denote this as $\partial_{\theta} \mathcal{L}(f_{\theta_1^{(t)}}, \tilde{f}_{\theta_2^{(t)}}; \mathcal{B})$ for brevity. Then, we clip the mini-batch gradient with a clipping threshold $c > 0$. Let $h^{(t)} = \min\{1, c/\|\partial_{\theta} \mathcal{L}(f_{\theta_1^{(t)}}, \tilde{f}_{\theta_2^{(t)}}; \mathcal{B}^{(t)})\|_F\}$, and we update $\theta^{(t)}$ as follows:

$$\theta^{(t+1)} = \theta^{(t)} - \eta \left\{ h^{(t)} \partial_{\theta} \mathcal{L}(f_{\theta_1^{(t)}}, \tilde{f}_{\theta_2^{(t)}}; \mathcal{B}^{(t)}) + \sigma c \Gamma^{(t)} \right\},$$

where $\eta > 0$ is the learning rate and $\text{vec}(\Gamma^{(t)}) \sim N(0, I_{rd})$ is the noise added to ensure differential privacy. We formally present the algorithm in 1.

Algorithm 1 DP-CLIP

- 1: **Input:** observed pairs of data $\{(x_i, \tilde{x}_i)\}_{i=1}^n$, number of iterations T , noise scale σ , clipping threshold c , learning rate η , mini-batch size b , initial parameters $\theta = (\theta_1^{(0)}, \theta_2^{(0)})$.
 - 2: **for** $t \in \{0, \dots, T-1\}$ **do**
 - 3: Uniformly sample mini-batch $\mathcal{B}^{(t)}$ of size b from $[n]$.
 - 4: **Compute mini-batch gradient** $g^{(t)} \leftarrow \partial_{\theta} \mathcal{L}(f_{\theta_1^{(t)}}, \tilde{f}_{\theta_2^{(t)}}; \mathcal{B})$.
 - 5: **Clip Gradient** $\bar{g}^{(t)} \leftarrow \min\{1, c/\|g^{(t)}\|_F\} g^{(t)}$.
 - 6: **Add Noise** $\tilde{g}^{(t)} \leftarrow \bar{g}^{(t)} + \sigma c \mathcal{N}(0, I)$.
 - 7: **Descent** $\theta^{(t+1)} \leftarrow \theta^{(t)} - \eta \tilde{g}^{(t)}$.
 - 8: **end for**
 - 9: **return** $\theta^{(T)}$
-

We show that this algorithm is differentially private. In particular, the following result suggests that by carefully choosing σ , it can achieve desired differential privacy guarantee.

Lemma 3.1. *There exists universal constants $C_{\epsilon}, C_{\sigma} > 0$ such that for $b < n/10$, DP-CLIP is (ϵ, δ) -differentially private for any $\epsilon \leq C_{\epsilon} b^2 T / n^2$ and $\delta > 0$ if we choose $\sigma \geq C_{\sigma} \sqrt{T \log(1/\delta) / (n\epsilon)}$.*

The proof is deferred to the Appendix.

4 Experiments

In this section, we evaluate our DP-CLIP on image classification and visual question answering tasks. We first introduce the training details in Section 4.1, then we provide a detailed experimental analysis on our method in Section 4.2 and Section 4.3. Our code is available at <https://github.com/dpclip/dpclip.git>.

4.1 Experiments Setup

For image classification, we use the pretrained CLIP, and then, for each of the four datasets listed below, we finetune on the training set using DP-CLIP and report the accuracy on the testing set. For each image, we

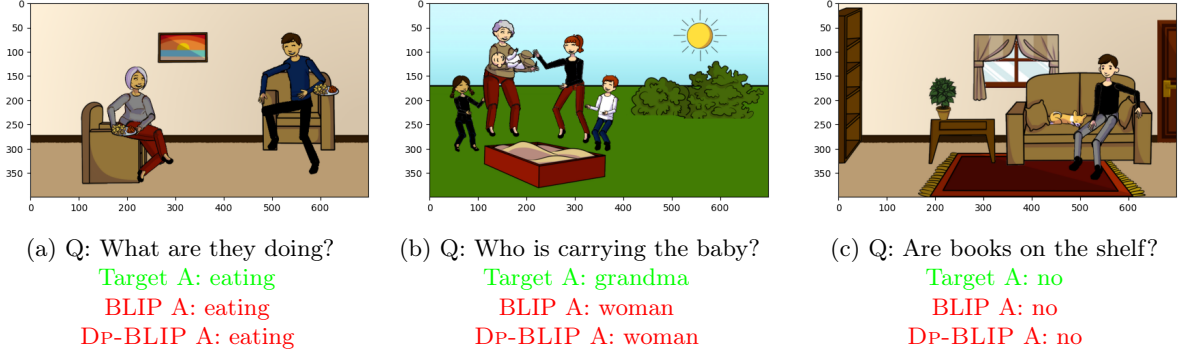


Figure 2: Example of visual question answering by BLIP and DP-BLIP

encode the image using CLIP’s image encoder and then encode each of the text of the classes with prompt using CLIP’s text encoder. We calculate the cosine similarity between the image and text encoders for classes. The predicted class is the one with the highest cosine similarity, following Radford et al. (2021).

We demonstrate that our DP-CLIP can be applied to a broad class of Vision-Language Pre-training models. To this end, for visual question answering, we use the pre-trained *Bootstrapping Language Image Pre-training* (BLIP) Li et al. (2022a), which achieves state-of-the-art performance on a wide range of vision-language tasks, as the backbone. The detailed background of BLIP is deferred to Appendix A. We apply the same framework, the per-batch gradient clipping and noise addition process, described in Algorithm 1 on BLIP, while using a different loss function. We call this DP-BLIP.

For simplicity, we focus on VQA problems within abstract scenes, where the questions and answers are restricted to abstract elements, as illustrated in Figure 2.

Datasets For image classification, we consider four benchmark image classification datasets, namely MNIST (LeCun et al., 1998), Fashion-MNIST (Xiao et al., 2017), CIFAR-10 (Krizhevsky, 2009), and SVHN (Netzer et al., 2011). MNIST is a collection of greyscale images belonging to handwritten digits, with a training set of 60,000 images and a test set of 10,000 images. Fashion-MNIST is a collection of greyscale images of fashion products belonging to 10 categories, with a training set of 60,000 images and a test set of 10,000 images. CIFAR-10 is a collection of color images belonging to one of 10 classes, such as airplane, automobile, and bird, with a training set of 60,000 images and a test set of 10,000 images. Finally, SVHN is a collection of color images representing street house view numbers, which are images of printed digits of house number plates. We use the training set of 73,257 samples and extra set of 531,131 samples for training, and using testing set of 26,032 samples for evaluation, where the evaluation metric is the classification accuracy.

For visual question answering, we consider the scene VQA2.0 dataset (Antol et al., 2015), which is a collection of abstract scene images along with questions and answers, with a training set of 20k images with 60k questions-answers and a test set of 10k images with 30k questions-answers. We use exact-match accuracy as our primary evaluation metric, following Li et al. (2022a, 2021a), which measures the proportion of correct answers given by our model.

Model Architecture For image classification, the base model is OpenAI’s CLIP model pretrained on the ImageNet dataset (Deng et al., 2009). It consist of a *ViT-L/14-336px* Transformer architecture as an image encoder and a masked self-attention Transformer as a text encoder. The vision Transformer consists of 24 layers with width of 1024 and 16 heads. The text Transformer consists of 12 layers with width of 768 and 12 heads.

For visual question answering, the base model is BLIP pretrained on two human-annotated datasets, COCO (Lin et al., 2014) and Visual Genome (Krishna et al., 2017), and three web datasets, Conceptual Captions (Sharma et al., 2018), Conceptual 12M (Changpinyo et al., 2021), and SBU captions (Ordonez

et al., 2011), consisting of an unimodal image encoder, an image-grounded text encoder and an answer decoder, as illustrated in Figure 3.

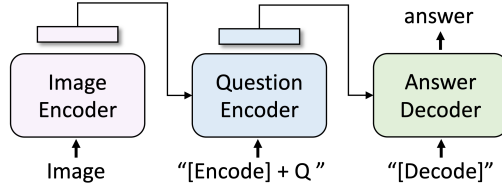


Figure 3: Structure of BLIP for VQA Li et al. (2022a)

Training Details The value of the noise multiplier, σ , is determined by the size of the training set n , the batch size b , the number of iterations T , and privacy parameters (ϵ, δ) . Lemma 3.1 provides a guidance on the choice of these parameters. We use TensorFlow Privacy¹ for privacy accounting. Throughout the experiments, we set $\delta = 1/2n$ where n is the size of the training set.

To obtain optimal results, we conduct hyperparameter tuning and prompt engineering. Because the baseline methods in Papernot et al. (2020) and Vinaroz and Park (2023) did not account for the privacy loss on tuning, we do the same to ensure a fair comparison. We set the learning rate $\eta = 10^{-5}$, since we find it yields the best performance across the datasets. We vary the clipping threshold c from 0.1 to 1, and batch size b from 16 to 128. We train the model for 15 to 30 epochs. Regarding prompt engineering, we employ the prompts provided in the CLIP GitHub repository². Our experiments indicated that the inclusion of these prompts enhanced the accuracy of our model by 1 – 2%.

All our models are implemented in PyTorch (Paszke et al., 2019) using one NVIDIA A100 80G GPU.

4.2 Image Classification Results

Table 1: Evaluation of the Classification Accuracy vs. Privacy of DP-CLIP

	MNIST	Fashion-MNIST	CIFAR-10	SVHN
$\epsilon = 10$	98.78	91.52	95.74	93.69
$\epsilon = 3$	98.56	91.27	95.62	93.23
$\epsilon = 1$	98.44	90.65	94.81	92.92
$\epsilon = 0.5$	98.40	90.02	94.47	91.03
$\epsilon = 0.25$	95.62	89.09	93.51	87.65

We present the classification accuracy of DP-CLIP on the four datasets under various ϵ in table 1. We observe that DP-CLIP is able to recover features under the regime with stringent privacy parameters. In particular, for all datasets, $\epsilon = 1$ performs within 1% of $\epsilon = 10$, which indicates the strong potential of DP-CLIP to offer better privacy guarantees while maintaining utility.

To further evaluate the performance of DP-CLIP, we compare our DP-CLIP against other state-of-the-art differentially private image classification methods. We consider DP-Sinkhorn (Cao et al., 2021), DP-KIP (Vinaroz and Park, 2023), DP-SGD with Tempered Sigmoid (Papernot et al., 2020), Private-kNN (Zhu et al., 2020), and Active Learning (Zhao et al., 2019). We present the comparisons in Table 2 below. For brevity, only the best results from each paper are included.

From Table 2, we can see that for all $\epsilon \geq 1$, DP-CLIP outperforms all other methods on all four datasets while a smaller or equal ϵ . The most notable improvement is observed in the CIFAR-10 dataset, where

¹<https://github.com/tensorflow/privacy>

²<https://github.com/openai/CLIP>.

Table 2: Comparison with state-of-the-art DP methods on MNIST, FashionMNIST, CIFAR-10 and SVHN, with varying privacy parameter ϵ . DP-SGD (TS) stands for DP-SGD with Tempered Sigmoid.

MNIST			Fashion-MNIST		
	ϵ	Accuracy		ϵ	Accuracy
DP-Sinkhorn	10	83.2	DP-Sinkhorn	10	73.0
DP-KIP	10	97.96	DP-KIP	10	90.2
DP-CLIP	10	98.78	DP-CLIP	10	91.52
Active Learning	3	97.3			
DP-CLIP	3	98.56			
DP-SGD (TS)	2.93	98.1	DP-SGD (TS)	2.7	86.1
DP-KIP	1	97.78	DP-KIP	1	88.3
DP-CLIP	1	98.44	DP-CLIP	1	90.65
Private-kNN	0.47	98.8			
DP-CLIP	0.5	98.40			

CIFAR-10			SVHN		
	ϵ	Accuracy		ϵ	Accuracy
DP-SGD (TS)	7.53	66.2	Active Learning	6	85.0
DP-CLIP	3	95.62	DP-CLIP	3	91.75
Private-kNN	2.92	70.8	Private-kNN	0.49	91.6
DP-CLIP	1	94.81	DP-CLIP	0.5	91.03

our DP-CLIP achieves 20 \sim 30% increase in performance. This indicates our method has the potential to overcome the training diverging issue for large datasets by directly applying DP-SGD to diffusion models (Carlini et al., 2023). Although the performance of Private-kNN is comparable to DP-CLIP on the MNIST and SVHN datasets when $\epsilon < 0.5$. Our DP-CLIP offers more flexibility compared to Private-kNN, as it is only for classification tasks, whereas DP-CLIP can be used for a variety of more complex downstream tasks.

4.3 VQA Results

Visual Question Answering (VQA) has been increasingly used in many fields, such as healthcare, education, and social media (Srivastava et al., 2021). In Visual Question Answering (VQA), an image (I) is provided along with a related question (Q) in natural language form, and the goal is to generate accurate and meaningful answers (A). However, the images and text data used in training may contain sensitive information, and it is of paramount importance to ensure privacy preservation measures are in place (Bara et al., 2022). To our best knowledge, we are the first to introduce differential privacy to VQA tasks.

The goal of the experiment in this section is to demonstrate that adding DP noise does not significantly impact the accuracy of the results, compared to the non-private method, when all other parameters are held constant. The objective is not to fine-tune the model to compete with non-private state-of-the-art results, but rather to showcase that our approach achieves a comparable level of accuracy without compromising privacy. We note that BLIP can achieve state-of-the-art results on VQA with a much higher accuracy rate of 78.25% (Li et al., 2022a). However, in our study, we deliberately refrain from extensive parameter optimization and instead focus on providing a baseline analysis. As a result, we report lower accuracy results compared to the fine-tuned BLIP approach. From Table 3, we can see that our model maintains utility even as privacy measures are increased, suggesting its resilience to noise. We defer more experimental results on this task to Appendix A.

Table 3: Evaluation of VQA on the abstract scene VQA2.0 dataset of DP-BLIP.

$\epsilon = \infty$ (non-private)	$\epsilon = 10$	$\epsilon = 3$	$\epsilon = 1$	$\epsilon = 0.5$
55.22%	52.95%	52.94%	52.94%	52.94%

5 Theoretical Analysis of DP-CLIP

In this section, we analyze the feature learning capacity of DP-CLIP and derive the privacy-utility trade-off under the linear representation and loss setting. Such a simplified setting has been commonly used in the deep learning theory literature to shed light on understanding complicated deep learning phenomena. For example, the linearized loss function for analyzing representation learning has been used in metric learning (Schroff et al., 2015; He et al., 2018), contrastive learning (Ji et al., 2021) and multimodal contrastive learning (Won et al., 2021; Alsan et al., 2021; Nakada et al., 2023). The linear representation setting has been widely adopted in transfer learning and self-supervised learning (Jing et al., 2021; Tian et al., 2021; Ji et al., 2021; Wu et al., 2022; Tian, 2022; Nakada et al., 2023).

Concretely, suppose that we observe pairs of data $\{(x_i, \tilde{x}_i)\}_{i=1}^n \subset \mathbb{R}^{d_1} \times \mathbb{R}^{d_2}$. We train dual *linear representations* $f(x) = G_1x$ and $\tilde{f}(x) = G_2x$, where $G_1 \in \mathbb{R}^{r \times d_1}$ and $G_2 \in \mathbb{R}^{r \times d_2}$, simultaneously with the following contrastive linear loss through noisy gradient descent. For notational brevity, let $G \triangleq [G_1, G_2] \in \mathbb{R}^{r \times d}$, where $d \triangleq d_1 + d_2$.

We aim to obtain G_1 and G_2 that minimize the following linearized loss function:

$$\mathcal{L}_L(G_1, G_2) = -\frac{1}{n} \sum_i \langle G_1x_i, G_2\tilde{x}_i \rangle + \frac{1}{n(n-1)} \sum_{i \neq j} \langle G_1x_i, G_2\tilde{x}_j \rangle + \Pi(G), \quad (5.1)$$

where the penalty term $\Pi(G) \triangleq (\alpha/4)\|GG^\top - I\|_F^2$ with $\alpha > 0$ is added to normalize G . Note that the CLIP loss 2.2 becomes equivalent to loss 5.1 without penalty when $\tau \rightarrow \infty$.

For observed data $\{(x_i, \tilde{x}_i)\}_{i=1}^n \subset \mathbb{R}^{d_1+d_2}$, we consider the following spiked covariance model(Johnstone, 2001; Bai and Yao, 2012; Yao et al., 2015; Zhang et al., 2018; Zeng et al., 2019; Ji et al., 2021; Nakada et al., 2023) as the data generation process.

$$x_i = U_1^* z_i + \xi_i, \quad \tilde{x}_i = U_2^* z_i + \tilde{\xi}_i, \quad (5.2)$$

where U_1^* and U_2^* are orthonormal matrices. Since the model equation 5.2 is only identifiable up to rotation, we assume that Σ_z is a diagonal matrix. Without loss of generality, we further assume that $\|\Sigma_z\| = 1$. We assume that z_i , ξ_i and $\tilde{\xi}_i$ are mean 0 sub-Gaussian random variables with parameters bounded by a universal constant. Furthermore, we assume the independence of variables; $z_i \perp \xi_i$, $\tilde{z}_i \perp \tilde{\xi}_i$, and $\xi_i \perp \tilde{\xi}_i$.

There have been several works on analyzing the convergence of DP-SGD (Abadi et al., 2016) with per-sample clipping (Yu et al., 2019; Bassily et al., 2019; Feldman et al., 2020; Chen et al., 2020a; Yang et al., 2022; Bu et al., 2022; Fang et al., 2023). Closely related works are Yang et al. (2022) and Fang et al. (2023). However, the contrastive loss function of CLIP cannot be decomposed into the sum of per-sample losses, since CLIP learns by contrasting modalities across sampled pairs. This is the reason why DP-CLIP employs per-*mini-batch* clipping. In addition, in spite of the linearization, our loss function equation 5.1, like the original CLIP loss, is neither convex nor globally Lipschitz, which makes the theoretical analysis highly nontrivial.

5.1 Privacy-utility Trade-off of DP-CLIP

Let G_1^*, G_2^* be the minimizer of the population loss $\mathbb{E}[\mathcal{L}_L(G)]$. For simplicity, we assume the regularization parameter $\alpha = \Theta(1)$ is of constant order. Since pre-trained encoder is often used in downstream tasks, where the output of the encoder is fed into neural networks or linear probes, the essential information of the learned representation is contained in the linear transformation. For this reason, we measure the

performance of the learned representations G_1 and G_2 through the excess loss of information defined as $\min_{A \in \mathbb{R}^{r \times r}} \|AG_1 - G_1^*\|_F \vee \min_{A \in \mathbb{R}^{r \times r}} \|AG_2 - G_2^*\|_F$. For “good” encoders, we expect that a certain linear transformation of it is close to the representations obtained using infinite number of training samples.

Before presenting our results, we introduce notations. For two sequences of positive numbers $\{a_k\}_k$ and $\{b_k\}_k$, we write $a_k \lesssim b_k$ if and only if there exists a constant $C > 0$, independent of the index k , such that $\sup_{k \in \mathcal{K}} (a_k/b_k) < C$. Moreover, we write $a_k \ll b_k$ when $\sup_{k \in \mathcal{K}} (a_k/b_k) \leq C_u$ holds for a sufficiently large universal constant $C_u > 0$ common throughout the paper. For any matrix A , we denote $\|A\|$ and $\|A\|_F$ as the operator norm and Frobenius norm of A respectively. For any matrix A , let $\lambda_{\min}(A)$ and $\lambda_{\max}(A)$ be the minimum and maximum singular values of A , respectively. For any zero-mean random variable X , we define its covariance matrix as $\Sigma_X \triangleq \mathbb{E}[XX^\top]$. Let the signal-to-noise ratio for x and \tilde{x} be $s_1^2 \triangleq \|\Sigma_z\|/\|\Sigma_\xi\|$ and $s_2^2 \triangleq \|\Sigma_z\|/\|\Sigma_{\tilde{\xi}}\|$, respectively.

Assumption 5.1. Assume that $d > r$ and $n \gg r(r + s_1^{-2}r_e(\Sigma_\xi) + s_2^{-2}r_e(\Sigma_{\tilde{\xi}}))^2 \log^3(T(n+d))$, where r_e is the effective rank defined as $r_e(A) \triangleq \text{Tr}(A)/\|A\|$ for any square matrix A .

Assumption 5.2 (Signal-to-noise Ratio). Assume that $\min\{s_1^2, s_2^2\} \gtrsim 1$.

Assumption 5.3 (Signal Condition Number). Assume that $\kappa \triangleq \lambda_{\max}(\Sigma_z)/\lambda_{\min}(\Sigma_z) \lesssim 1$.

Assumption 5.1 ensures that we have an effective number of samples to separate the core signal from the noise. Assumption 5.2 is a mild condition on the signal-to-noise ratio. It allows the noise to be the same strength as signal. Assumption 5.3 ensures that core features are strongly shared between the two modalities.

Here we introduce the privacy-utility trade-off of DP-CLIP under linear loss.

Theorem 5.1 (Privacy-utility Trade-off). *Suppose Assumptions 5.1, 5.2 and 5.3 hold. Assume that $\alpha = \Theta(1)$. Let $G^{(T)}$ be the representation obtained from the algorithm 1 with loss $\mathcal{L}_L(G)$. Suppose that the initial representation $G^{(0)}$ satisfies $\min_{O \in \mathbb{R}^{r \times r}: O^\top O = I} \|OG^{(0)} - \hat{G}\|_F \ll 1$. Choose $c \gg 1$, $b = \lceil \nu n \rceil$, where $\nu \in (0, 1)$ is a constant. Also choose $\eta > 0$ and $\sigma > 0$ as*

$\eta = \{\sigma \sqrt{T(rd + \log(T(n+d)))}\}^{-1}$, $\sigma = C_\sigma \sqrt{T \log(1/\delta)/(n\epsilon)}$, where C_σ is a constant appearing in Lemma 3.1. Then, Algorithm 1 under loss \mathcal{L}_L is (ϵ, δ) -DP and for sufficiently large T ,

$$\begin{aligned} & \min_{A \in \mathbb{R}^{r \times r}} \|AG_1^{(T)} - G_1^*\|_F \vee \min_{A \in \mathbb{R}^{r \times r}} \|AG_2^{(T)} - G_2^*\|_F \\ & \lesssim \underbrace{\exp\left(-\frac{n\epsilon}{8\kappa C_\sigma \sqrt{\log(1/\delta)\{rd + \log(T(n+d))\}}}\right)}_{\text{optimization error}} + \underbrace{\frac{\log^{1/4}(1/\delta)\{rd + \log(T(n+d))\}^{1/4}}{\sqrt{n\epsilon}}}_{\text{the cost of privacy}} \\ & \quad + \underbrace{\sqrt{\frac{r(r + s_1^{-2}r_e(\Sigma_\xi) + s_2^{-2}r_e(\Sigma_{\tilde{\xi}}))^2 \log^3(n+d)}{n}}}_{\text{statistical error}}. \end{aligned} \tag{5.3}$$

holds with probability at least $1 - O((n+d)^{-1})$.

Proof Outline of Theorem 5.1. This result follows from the linear convergence result (Theorem B.1) of Algorithm 1; we can bound the distance between $G^{(T)}$ and the global minimizer of the loss \mathcal{L}_L by three components, a linear converging term, the error from the injected noise, and the error from subsampling. To show this result, we first derive the one-step linear convergence bound for non-stochastic gradient descent without noise injection. To this end, we use the fact that \mathcal{L}_L is locally strongly convex and directionally smooth around its global minimum. For noisy stochastic gradient descent, we need to control the accumulation of errors coming from both privacy noise and subsampling. For this purpose, we exploit the fact that $\partial_G \mathcal{L}_L(G^{(t)}; \mathcal{B}^{(t)})$, a mini-batch gradient of \mathcal{L}_L evaluated at $G^{(t)}$, is an unbiased estimator of $\partial_G \mathcal{L}_L(G^{(t)})$, and control the deviation of the accumulated errors through the martingale concentration inequality. The accumulated error from subsampling is controlled by the Bernstein concentration bound from Bardenet and Maillard (2015), which turns out to be negligible since the batch size is chosen to be proportional to the number of samples. Given the linear convergence result, we set the value of η and σ as specified in Lemma

3.1 to conclude the proof. The proof and more detailed statement of Theorem 5.1 that specifies the exact condition on T is available in Corollary B.2 in the appendix.

In equation 5.3, the right-hand side consists of three terms: optimization error, privacy cost, and statistical error. The optimization error decreases exponentially in n , since the loss function \mathcal{L}_L behaves well locally around the global minimum. This term grows with T because the algorithm runs in two stages: in the first stage, the error decreases exponentially in T (see details in Theorem B.1), and in the second stage, when $G^{(T)}$ reaches a certain stable region, the optimization error starts to increase (slowly) if we continue to run more gradient descent updates. We also note that the optimization error is dominated by the term for the cost of privacy when $n\epsilon/\sqrt{\log(1/\delta)}$ is large. The second term corresponds to the additional cost to preserve privacy. Ignoring the logarithmic term $\log(T(n+d))$, the cost increases proportionally to $\log^{1/4}(1/\delta)/\epsilon^{1/2}$. This rate also appears similarly in Chen et al. (2020a); Yang et al. (2022); Fang et al. (2023) for the analysis of DP-SGD. Our technical analysis differs from theirs as they consider per-sample clipping for loss functions that satisfy certain smoothness condition, which does not hold for our loss 5.1. We also note that the loss 5.1 is not decomposable to apply per-sample clipping. Also, similar privacy cost bounds appear in the convergence analysis of differentially private gradient descent and related algorithms (Wang et al., 2017, 2019; Zhang et al., 2019; Wang et al., 2020; Cai et al., 2021, 2023). The statistical error term is due to the irreducible error coming from finite samples. The term depends on $r + s_1^{-2}r_e(\Sigma_\xi) + s_2^{-2}r_e(\Sigma_{\tilde{\xi}})$, which is trivially bounded by $O(r+d)$ under Assumption 5.2. When either the effective rank of noise covariance is small or the signal-to-noise ratio is large, the statistical error term becomes small.

Remark 5.1. In the analysis, the intrinsic dimension r of the input data is assumed to be known. In practical situation, we can either choose r based on certain metric such as cross validation in downstream tasks, or estimate r based on the spectral decay of the cross-covariance matrix.

Remark 5.2. The initial value condition is satisfied if $\min_{O:O^\top O=I} \|OG^{(0)} - \hat{G}\| \ll 1/\sqrt{r}$. Thus the condition is considered to be weak when r is small. As in our experiments in Section 4, we can employ initial representations trained with non-private optimizers with certain number of samples.

6 Discussion

In this paper, we introduced DP-CLIP, a novel approach that integrates differential privacy into the CLIP to address privacy concerns associated with vision-language tasks. Our experiments demonstrated that DP-CLIP outperforms other state-of-the-art differentially private classification methods. To the best of our knowledge, we first introduce differential privacy into VQA tasks, by our DP-BLIP. Our experiment showed that the performance is comparable to the non-private BLIP, which highlights the robustness of multimodal contrastive models to the noise introduced to preserve privacy. In addition, we theoretically proved the convergence of our algorithm under linear representation settings, and presented a privacy-utility trade-off for DP-CLIP in the situation where gradients are clipped per batch and the loss function does not satisfy the smoothness conditions such as Lipschitz smoothness.

Our work also points to several directions that need further investigation. We leave further experiments on privatizing other multimodal models and evaluate them on a wider range of vision-language downstream tasks (such as visual entailment or image-text retrieval (Li et al., 2021a)) as future work. Moreover, our theoretical analysis follows the current machine learning literature and studied the linear representation functions. The analysis on non-linear representations remains a future work. Furthermore, Vyas et al. (2023) recently proposed a theoretical copyright protection framework for generative models, which is closely related to differential privacy as a mathematical measurement. As our method learns differentially private image representations, it can be potentially used to generate images that protect copyright infringement, which we also leave as future work.

References

- Abadi, M., Chu, A., Goodfellow, I., McMahan, H. B., Mironov, I., Talwar, K., and Zhang, L. (2016). Deep learning with differential privacy. In *Proceedings of the 2016 ACM SIGSAC conference on computer and communications security*, pages 308–318.
- Alsan, H. F., Yıldız, E., Safdil, E. B., Arslan, F., and Arsan, T. (2021). Multimodal retrieval with contrastive pretraining. In *2021 International Conference on INnovations in Intelligent SysTems and Applications (INISTA)*.
- Antol, S., Agrawal, A., Lu, J., Mitchell, M., Batra, D., Zitnick, C. L., and Parikh, D. (2015). VQA: Visual Question Answering. In *International Conference on Computer Vision (ICCV)*.
- Bai, Z. and Yao, J. (2012). On sample eigenvalues in a generalized spiked population model. *Journal of Multivariate Analysis*.
- Bara, C.-P., Ping, Q., Mathur, A., Thattai, G., MV, R., and Sukhatme, G. S. (2022). Privacy preserving visual question answering. *arXiv preprint arXiv:2202.07712*.
- Bardenet, R. and Maillard, O.-A. (2015). Concentration inequalities for sampling without replacement. *Bernoulli*.
- Bassily, R., Feldman, V., Talwar, K., and Guha Thakurta, A. (2019). Private stochastic convex optimization with optimal rates. *Advances in Neural Information Processing Systems (NIPS)*.
- Basu, P., Roy, T. S., Naidu, R., Muftuoglu, Z., Singh, S., and Miresghallah, F. (2021). Benchmarking differential privacy and federated learning for bert models. *ArXiv*, abs/2106.13973.
- Beck, A. (2017). *First-order methods in optimization*. SIAM.
- Bu, Z., Wang, H., and Long, Q. (2021). On the convergence and calibration of deep learning with differential privacy. *arXiv preprint arXiv:2106.07830*.
- Bu, Z., Wang, Y.-X., Zha, S., and Karypis, G. (2022). Automatic clipping: Differentially private deep learning made easier and stronger. *arXiv preprint arXiv:2206.07136*.
- Bun, M., Dwork, C., Rothblum, G. N., and Steinke, T. (2018). Composable and versatile privacy via truncated cdp. In *Proceedings of the 50th Annual ACM SIGACT Symposium on Theory of Computing*, pages 74–86.
- Cai, T. T., Wang, Y., and Zhang, L. (2021). The cost of privacy: Optimal rates of convergence for parameter estimation with differential privacy. *The Annals of Statistics*, 49(5):2825–2850.
- Cai, T. T., Wang, Y., and Zhang, L. (2023). Score attack: A lower bound technique for optimal differentially private learning. *arXiv preprint arXiv:2303.07152*.
- Cao, T., Bie, A., Vahdat, A., Fidler, S., and Kreis, K. (2021). Don’t generate me: Training differentially private generative models with sinkhorn divergence. In *Advances in Neural Information Processing Systems (NIPS)*.
- Carlini, N., Hayes, J., Nasr, M., Jagielski, M., Sehwag, V., Tramèr, F., Balle, B., Ippolito, D., and Wallace, E. (2023). Extracting training data from diffusion models. *arXiv preprint arXiv:2301.13188*.
- Changpinyo, S., Sharma, P., Ding, N., and Soricut, R. (2021). Conceptual 12m: Pushing web-scale image-text pre-training to recognize long-tail visual concepts. In *Proceedings of the IEEE/CVF Conference on Computer Vision and Pattern Recognition*, pages 3558–3568.
- Chen, X., Wu, S. Z., and Hong, M. (2020a). Understanding gradient clipping in private sgd: A geometric perspective. *Advances in Neural Information Processing Systems (NIPS)*.

- Chen, Y.-C., Li, L., Yu, L., El Kholy, A., Ahmed, F., Gan, Z., Cheng, Y., and Liu, J. (2020b). Uniter: Universal image-text representation learning. In *Computer Vision – ECCV 2020: 16th European Conference, Glasgow, UK, August 23–28, 2020, Proceedings, Part XXX*, page 104–120, Berlin, Heidelberg. Springer-Verlag.
- Chi, Y., Lu, Y. M., and Chen, Y. (2019). Nonconvex optimization meets low-rank matrix factorization: An overview. *IEEE Transactions on Signal Processing*.
- Deng, J., Dong, W., Socher, R., Li, L.-J., Li, K., and Fei-Fei, L. (2009). Imagenet: A large-scale hierarchical image database. In *Proceedings of the IEEE Conference on Computer Vision and Pattern Recognition (CVPR)*.
- Dorbala, V. S., Sigurdsson, G. A., Piramuthu, R., Thomason, J., and Sukhatme, G. S. (2022). Clip-nav: Using clip for zero-shot vision-and-language navigation. In *Proceedings of Conference on Robot Learning*.
- Dwork, C., McSherry, F., Nissim, K., and Smith, A. (2006). Calibrating noise to sensitivity in private data analysis. In *Proceedings of Theory of Cryptography Conference (TCC)*.
- Dwork, C., Roth, A., et al. (2014). The algorithmic foundations of differential privacy. *Foundations and Trends® in Theoretical Computer Science*, 9(3–4):211–407.
- Fang, H., Li, X., Fan, C., and Li, P. (2023). Improved convergence of differential private sgd with gradient clipping. In *Proceedings of the International Conference on Learning Representations (ICLR)*.
- Feldman, V., Koren, T., and Talwar, K. (2020). Private stochastic convex optimization: optimal rates in linear time. In *Proceedings of ACM SIGACT Symposium on Theory of Computing (STC)*.
- Galatolo, F., Cimino, M., and Vaglini, G. (2021). Generating images from caption and vice versa via clip-guided generative latent space search. *Proceedings of the International Conference on Image Processing and Vision Engineering*.
- Gan, Z., Li, L., Li, C., Wang, L., Liu, Z., and Gao, J. (2022). Vision-language pre-training: Basics, recent advances, and future trends. *Found. Trends. Comput. Graph. Vis.*, 14(3–4):163–352.
- Gao, S. and Ma, Z. (2021). Sparse gca and thresholded gradient descent. *arXiv preprint arXiv:2107.00371*.
- He, X. and Zhang, Y. (2021). Quantifying and mitigating privacy risks of contrastive learning. *CCS*, pages 845–863.
- He, X., Zhou, Y., Zhou, Z., Bai, S., and Bai, X. (2018). Triplet-center loss for multi-view 3d object retrieval. In *Proceedings of the IEEE Conference on Computer Vision and Pattern Recognition (CVPR)*.
- Hoory, S., Feder, A., Tendler, A., Cohen, A., Erell, S., Laish, I., Nakhost, H., Stemmer, U., Benjamini, A., Hassidim, A., and Matias, Y. (2021). Learning and evaluating a differentially private pre-trained language model. In *PRIVATENLP*.
- Imtiaz, H. and Sarwate, A. D. (2017). Differentially-private canonical correlation analysis. In *Proceedings of the IEEE Global Conference on Signal and Information Processing (GlobalSIP)*.
- Ji, W., Deng, Z., Nakada, R., Zou, J., and Zhang, L. (2021). The power of contrast for feature learning: A theoretical analysis. *arXiv preprint arXiv:2110.02473*.
- Jing, L., Vincent, P., LeCun, Y., and Tian, Y. (2021). Understanding dimensional collapse in contrastive self-supervised learning. *arXiv preprint arXiv:2110.09348*.
- Johnstone, I. M. (2001). On the distribution of the largest eigenvalue in principal components analysis. *Annals of Statistics*.

- Kiros, R., Salakhutdinov, R., and Zemel, R. (2014). Multimodal neural language models. In *International conference on machine learning*, pages 595–603. PMLR.
- Krishna, R., Zhu, Y., Groth, O., Johnson, J., Hata, K., Kravitz, J., Chen, S., Kalantidis, Y., Li, L.-J., Shamma, D. A., et al. (2017). Visual genome: Connecting language and vision using crowdsourced dense image annotations. *International journal of computer vision*, 123:32–73.
- Krizhevsky, A. (2009). Learning multiple layers of features from tiny images. In *Tech Report*.
- Laurent, B. and Massart, P. (2000). Adaptive estimation of a quadratic functional by model selection. *Annals of Statistics*.
- LeCun, Y., Bottou, L., Bengio, Y., and Haffner, P. (1998). Gradient-based learning applied to document recognition. In *Proceedings of the IEEE*.
- Li, J., Li, D., Xiong, C., and Hoi, S. (2022a). Blip: Bootstrapping language-image pre-training for unified vision-language understanding and generation. In *ICML*.
- Li, J., Selvaraju, R. R., Gotmare, A. D., Joty, S., Xiong, C., and Hoi, S. (2021a). Align before fuse: Vision and language representation learning with momentum distillation. In Beygelzimer, A., Dauphin, Y., Liang, P., and Vaughan, J. W., editors, *Advances in Neural Information Processing Systems*.
- Li, K., Zhang, Y., Li, K., Li, Y., and Fu, Y. (2019). Visual semantic reasoning for image-text matching. In *2019 IEEE/CVF International Conference on Computer Vision (ICCV)*, pages 4653–4661.
- Li, X., Tramer, F., Liang, P., and Hashimoto, T. (2021b). Large language models can be strong differentially private learners. In *Proceedings of International Conference on Learning Representations (ICLR)*.
- Li, X., Tramer, F., Liang, P., and Hashimoto, T. (2022b). Large language models can be strong differentially private learners. In *International Conference on Learning Representations*.
- Li, X., Yin, X., Li, C., Hu, X., Zhang, P., Zhang, L., Wang, L., Hu, H., Dong, L., Wei, F., Choi, Y., and Gao, J. (2020). Oscar: Object-semantics aligned pre-training for vision-language tasks. *ECCV 2020*.
- Li, Y., Liang, F., Zhao, L., Cui, Y., Ouyang, W., Shao, J., Yu, F., and Yan, J. (2021c). Supervision exists everywhere: A data efficient contrastive language-image pre-training paradigm. *arXiv preprint arXiv:2110.05208*.
- Lin, T.-Y., Maire, M., Belongie, S., Hays, J., Perona, P., Ramanan, D., Dollár, P., and Zitnick, C. L. (2014). Microsoft coco: Common objects in context. In *Computer Vision–ECCV 2014: 13th European Conference, Zurich, Switzerland, September 6–12, 2014, Proceedings, Part V 13*, pages 740–755. Springer.
- Liu, H., Jia, J., Qu, W., and Gong, N. Z. (2021). Encodermi: Membership inference against pre-trained encoders in contrastive learning. *CCS*, pages 2081 – 2095.
- Nakada, R., Gulluk, H. I., Deng, Z., Ji, W., Zou, J., and Zhang, L. (2023). Understanding multimodal contrastive learning and incorporating unpaired data. *arXiv preprint arXiv:2302.06232*.
- Narasimhan, M., Rohrbach, A., and Darrell, T. (2021). Clip-it! language-guided video summarization. *Advances in Neural Information Processing Systems*, 34:13988–14000.
- Netzer, Y., Wang, T., Coates, A., Bissacco, A., Wu, B., and Ng, A. Y. (2011). Reading digits in natural images with unsupervised feature learning. In *NIPS Workshop on Deep Learning and Unsupervised Feature Learning*.
- Ordonez, V., Girish, K., and Tamara, B. (2011). Im2text: Describing images using 1 million captioned photographs. *NIPS*.

- Papernot, N., Thakurta, A., Song, S., Chien, S., and Erlingsson, Ú. (2020). Tempered sigmoid activations for deep learning with differential privacy. In *Theory and Practice of Differential Privacy*.
- Paszke, A., Gross, S., Massa, F., Lerer, A., Bradbury, J., Chanan, G., Killeen, T., Lin, Z., Gimelshein, N., Antiga, L., et al. (2019). Pytorch: An imperative style, high-performance deep learning library. *Advances in neural information processing systems*, 32.
- Peng Xu, Xiatian Zhu, D. A. C. (2022). Multimodal learning with transformers: A survey. *arXiv preprint arXiv:2206.06488*.
- Radford, A., Kim, J. W., Hallacy, C., Ramesh, A., Goh, G., Agarwal, S., Sastry, G., Askell, A., Mishkin, P., Clark, J., et al. (2021). Learning transferable visual models from natural language supervision. In *Proceedings of the International Conference on Machine Learning (ICML)*.
- Schroff, F., Kalenichenko, D., and Philbin, J. (2015). Facenet: A unified embedding for face recognition and clustering. In *Proceedings of the IEEE Conference on Computer Vision and Pattern Recognition (CVPR)*.
- Sharma, P., Ding, N., Goodman, S., and Soricut, R. (2018). Conceptual captions: A cleaned, hypernymed, image alt-text dataset for automatic image captioning. In *Proceedings of the 56th Annual Meeting of the Association for Computational Linguistics (Volume 1: Long Papers)*, pages 2556–2565.
- Srivastava, Y., Murali, V., Dubey, S. R., and Mukherjee, S. (2021). Visual question answering using deep learning: A survey and performance analysis. In *Computer Vision and Image Processing: 5th International Conference, CVIP 2020, Prayagraj, India, December 4-6, 2020, Revised Selected Papers, Part II* 5, pages 75–86. Springer.
- Tian, Y. (2022). Deep contrastive learning is provably (almost) principal component analysis. *arXiv preprint arXiv:2201.12680*.
- Tian, Y., Chen, X., and Ganguli, S. (2021). Understanding self-supervised learning dynamics without contrastive pairs. In *Proceedings of the International Conference on Machine Learning (ICML)*.
- Vinaroz, M. and Park, M. J. (2023). Differentially private kernel inducing points (dp-kip) for privacy-preserving data distillation. *arXiv preprint arXiv:2301.13389*.
- Vyas, N., Kakade, S., and Barak, B. (2023). Provable copyright protection for generative models. *arXiv preprint arXiv:2302.10870*.
- Wainwright, M. J. (2019). *High-dimensional statistics: A non-asymptotic viewpoint*. Cambridge university press.
- Wang, D., Chen, C., and Xu, J. (2019). Differentially private empirical risk minimization with non-convex loss functions. In *Proceedings of the International Conference on Machine Learning (ICML)*.
- Wang, D., Xiao, H., Devadas, S., and Xu, J. (2020). On differentially private stochastic convex optimization with heavy-tailed data. In *International Conference on Machine Learning*, pages 10081–10091. PMLR.
- Wang, D., Ye, M., and Xu, J. (2017). Differentially private empirical risk minimization revisited: Faster and more general. *Advances in Neural Information Processing Systems*, 30.
- Wang, Z., Codella, N., Chen, Y.-C., Zhou, L., Yang, J., Dai, X., Xiao, B., You, H., Chang, S.-F., and Yuan, L. (2022). Clip-td: Clip targeted distillation for vision-language tasks. *arXiv preprint arXiv:2201.05729*.
- Won, M., Oramas, S., Nieto, O., Gouyon, F., and Serra, X. (2021). Multimodal metric learning for tag-based music retrieval. In *Proceedings of the IEEE International Conference on Acoustics, Speech and Signal Processing (ICASSP)*.

- Wu, R., Zhang, L., and Tony Cai, T. (2022). Sparse topic modeling: Computational efficiency, near-optimal algorithms, and statistical inference. *Journal of the American Statistical Association*.
- Xiao, H., Rasul, K., and Vollgraf, R. (2017). Fashion-mnist: a novel image dataset for benchmarking machine learning algorithms. *arXiv preprint arXiv:1708.07747*.
- Xu, P., Zhu, X., and Clifton, D. A. (2022). Multimodal learning with transformers: A survey. *arXiv preprint arXiv:2206.06488*.
- Yang, X., Zhang, H., Chen, W., and Liu, T.-Y. (2022). Normalized/clipped sgd with perturbation for differentially private non-convex optimization. *arXiv preprint arXiv:2206.13033*.
- Yao, J., Zheng, S., and Bai, Z. (2015). *Sample covariance matrices and high-dimensional data analysis*. Cambridge University Press Cambridge.
- Yao, L., Huang, R., Hou, L., Lu, G., Niu, M., Xu, H., Liang, X., Li, Z., Jiang, X., and Xu, C. (2021). Filip: fine-grained interactive language-image pre-training. *arXiv preprint arXiv:2111.07783*.
- Yu, D., Naik, S., Backurs, A., Gopi, S., Inan, H. A., Kamath, G., Kulkarni, J., Lee, Y. T., Manoel, A., Wutschitz, L., Yekhanin, S., and Zhang, H. (2022). Differentially private fine-tuning of language models. In *International Conference on Learning Representations*.
- Yu, D., Zhang, H., Chen, W., Liu, T.-Y., and Yin, J. (2019). Gradient perturbation is underrated for differentially private convex optimization. *arXiv preprint arXiv:1911.11363*.
- Yu, Y., Wang, T., and Samworth, R. J. (2015). A useful variant of the davis–kahan theorem for statisticians. *Biometrika*.
- Zeng, X., Xia, Y., and Zhang, L. (2019). Double cross validation for the number of factors in approximate factor models. *arXiv preprint arXiv:1907.01670*.
- Zhang, A. R., Cai, T. T., and Wu, Y. (2018). Heteroskedastic pca: Algorithm, optimality, and applications. *arXiv preprint arXiv:1810.08316*.
- Zhang, J., He, T., Sra, S., and Jadbabaie, A. (2019). Why gradient clipping accelerates training: A theoretical justification for adaptivity. *arXiv preprint arXiv:1905.11881*.
- Zhao, Z., Papernot, N., Singh, S., Polyzotis, N., and Odena, A. (2019). Improving differentially private models with active learning. *arXiv preprint arXiv:1910.01177*.
- Zhu, Y., Yu, X., Chandraker, M., and Wang, Y.-X. (2020). Private-knn: Practical differential privacy for computer vision. In *Proceedings of the IEEE Conference on Computer Vision and Pattern Recognition (CVPR)*.

A Detailed Experimental Results

In this section, we provide additional experimental setups and results.

A.1 Image Classification

We present the hyperparameters used in image classification task in Table 4.

Table 4: Tuned Hyperparameters for Image Classification DP-CLIP

	MNIST	Fashion-MNIST	CIFAR-10	SVHN
lr	1e-05	1e-05	1e-05	1e-05
betas	(0.9, 0.98)	(0.9, 0.98)	(0.9, 0.98)	(0.9, 0.98)
eps	1e-06	1e-06	1e-06	1e-06
weight decay	0.01	1e-06	1e-06	1e-06
num epochs	30	30	30	15
batch size	32	32	32	32

A.2 VQA

The *Bootstrapping Language Image Pre-training* (BLIP) Li et al. (2022a) is a novel framework for VLP (Vision-Language Pre-training Gan et al. (2022)) that offers broad applicability to various downstream tasks. It introduces (a) *Captioning and Filtering* (CapFilt), a pioneering method for dataset bootstrapping that enables learning from noisy image-text pairs, and (b) *Multimodal mixture of Encoder-Decoder* (MED), which is a novel model architecture capable of functioning as a unimodal encoder, an image-grounded text encoder, or an image-grounded text decoder. This versatility facilitates effective multi-task pre-training and flexible transfer learning. The MED model is jointly pre-trained using three vision-language objectives: *image-text contrastive learning* (Radford et al., 2021) to align the vision and language representations, *image-text matching* (Li et al., 2019) to distinguish between positive and negative image-text pairs, and *image-conditioned language modeling* (Kiros et al., 2014) to generate good textual descriptions given an image. We decided to use BLIP as our backbone since it currently achieves state-of-the-art performance on the VQA task.

For VQA tasks, instead of framing it as a multi-answer classification problem Chen et al. (2020b); Li et al. (2020), BLIP takes a different approach by formulating it as an answer generation task (Li et al., 2021a, 2022a). This formulation allows for open-ended VQA, where the model generates answers rather than selecting from a predefined set of options, which is consistent with the task used in Li et al. (2022a) and Li et al. (2021a). As depicted in Figure 3, during the finetuning process, an image-question pair is encoded into multimodal embeddings, which are then fed into an answer decoder. The VQA model is fine-tuned using the language modeling (LM) loss, with ground-truth answers serving as targets, following the methodology outlined in the original paper.

We report the exact-match accuracy mentioned in 4.3, here, we additionally evaluate it using another metric that is robust to inter-human variability in phrasing the answers, introduced in <https://visualqa.org/evaluation.html>. The evaluation code was taken from ALBEF’s github repository, where we consider the top three answers given by humans to a question and our accuracy is taken to be $\min\{1, \# \text{ humans saying that answer}/3\}$ and we output the average accuracy over the training set. The following results, shown in Tab. 5, suggests our privacy-aware approach can achieve comparable performance to the non-private method.

Table 5: Evaluation of VQA on the abstract scene VQA2.0 dataset of DP-BLIP using modified accuracy metric

$\epsilon = \infty$ (non-private)	$\epsilon = 10$	$\epsilon = 3$	$\epsilon = 1$	$\epsilon = 0.5$
63.74%	62.44%	62.30%	62.28%	62.21%

B Proofs of Theoretical Results

Before going into the proofs, we introduce notations to be used in later sections.

B.1 Notation

In this section, we introduce notations to be used. We write $a_k = O(b_k)$ if $a_k \lesssim b_k$ holds and $a_k = \Omega(b_k)$ if $a_k \gtrsim b_k$ holds. $\mathbb{O}_{d,r} \triangleq \{O \in \mathbb{R}^{r \times d} : O^\top O = I_r\}$ as a set of orthogonal matrices of order $d \times r$. We write $a \vee b$ and $a \wedge b$ to denote $\max(a, b)$ and $\min(a, b)$, respectively. For any matrix A , let $\lambda_j(A)$ be the j -th largest singular value of A . Let $\lambda_{\min}(A)$ and $\lambda_{\max}(A)$ be the minimum and maximum singular values of A , respectively. Moreover, for any square matrix A , define its effective rank as $r_e(A) = \text{Tr}(A)/\|A\|$. For any zero-mean random variables X and \tilde{X} , we define the covariance matrix of X as $\Sigma_X \triangleq \mathbb{E}[XX^\top]$, and the cross-covariance matrix of X and \tilde{X} as $\Sigma_{X,\tilde{X}} \triangleq \mathbb{E}[X\tilde{X}^\top]$. Define $\hat{\Sigma}_{x,\tilde{x}}$ as $\hat{\Sigma}_{x,\tilde{x}} \triangleq 1/n \sum_{i \in [n]} x_i \tilde{x}_i^\top - 1/n/(n-1) \sum_{i \neq j} x_i \tilde{x}_j^\top$.

Here we prove results in 5. We consider minimizing the following linear loss function:

$$\mathcal{L}_L(G) \triangleq -\text{tr}\left(G_1 \hat{\Sigma}_{x,\tilde{x}} G_2^\top\right) + \Pi(G),$$

where $\Pi(G) = (\alpha/4)\|GG^\top - I_r\|_F^2$ with $\alpha > 0$. We also define the loss for mini-batch \mathcal{B} as $\mathcal{L}_L(G; \mathcal{B}) \triangleq -\text{tr}\left(G_1 \hat{\Sigma}_{x,\tilde{x},\mathcal{B}} G_2^\top\right) + \Pi(G)$, where

$$\hat{\Sigma}_{x,\tilde{x},\mathcal{B}} \triangleq \frac{1}{|\mathcal{B}|} \sum_{i \in \mathcal{B}} x_i \tilde{x}_i^\top - \frac{1}{|\mathcal{B}|(|\mathcal{B}| - 1)} \sum_{i \neq j; i, j \in \mathcal{B}} x_i \tilde{x}_j^\top.$$

B.2 Differential Privacy of DP-CLIP

Here we present the Gaussian mechanism, the theoretical foundation of DP-SGD and DP-Adam above.

Definition 2 (Gaussian Mechanism). (*Dwork et al., 2014*) Let $f : \mathcal{X} \rightarrow \mathbb{R}^d$ be an arbitrary d -dimensional function, i.e. $f(x) = [f_1(x), f_2(x), \dots, f_d(x)]$ for $x \in \mathcal{X}$. Then, the Gaussian mechanism with parameter σ outputs,

$$M(x) = [f_1(x) + Z_1, f_2(x) + Z_2, \dots, f_d(x) + Z_d],$$

where $Z_i \sim \mathcal{N}(0, \sigma^2)$ for $i \in [d]$.

Definition 3 (ℓ_2 -sensitivity). The ℓ_2 -sensitivity of a function $f : \mathcal{X} \rightarrow \mathcal{Y}$ is defined as,

$$\Delta_2(f) = \max_{\text{adjacent } x_1, x_2 \in \mathcal{X}} \|f(x_1) - f(x_2)\|_2.$$

We then present the privacy guarantee for DP-CLIP.

Lemma B.1. There exists universal constants $C_\epsilon, C_\sigma > 0$ such that for $b < n/10$, DP-CLIP is (ϵ, δ) -differentially private for any $\epsilon \leq C_\epsilon b^2 T / n^2$ and $\delta > 0$ if we choose $\sigma \geq C_\sigma \sqrt{T \log(1/\delta)} / (n\epsilon)$.

Proof. Note that at each iteration, we can view Algorithm 1 as a repeated composition of subsampling and Gaussian mechanism. Let $\mathcal{M} = \mathcal{M}_T \circ \mathcal{M}_{T-1} \circ \dots \circ \mathcal{M}_1$, where $\mathcal{M}_t \triangleq \mathcal{M}_{t,G} \circ \mathcal{M}_{t,s}$ is the composition of subsampling and Gaussian mechanism at t -th iteration. We first bound the ℓ_2 sensitivity for Gaussian mechanism $\mathcal{M}_{t,G}$. Note that $\mathcal{M}_{t,G}$ depends on the mini-batch $\mathcal{B}^{(t)} \subset [n]$. We write $\bar{g}^{(t)} = \bar{g}^{(t)}((x_i, \tilde{x}_i)_{i \in \mathcal{B}^{(t)}})$ to make explicit the dependence of $g^{(t)}$ on the pairs of data $(x_i, \tilde{x}_i)_{i \in \mathcal{B}^{(t)}}$. Note that we can bound the ℓ_2 sensitivity as

$$\max_{i \in \mathcal{B}^{(t)}} \sup_{(x_i, \tilde{x}_i), (x'_i, \tilde{x}'_i) \in \mathbb{R}^{d_1+d_2}} |\bar{g}^{(t)}(\dots, (x_i, \tilde{x}_i), \dots) - \bar{g}^{(t)}(\dots, (x'_i, \tilde{x}'_i), \dots)| \leq 2c$$

due to per-batch clipping. The rest of the proof follows from the result of privacy amplification by subsampling (Theorem 11 from Bun et al. (2018)), and a similar argument in the proof of Lemma 3.1 from Yang et al. (2022). \square

B.3 Optimization Error Bound

In this subsection, we aim to derive the optimization error bound for $\text{dist}(G^{(T)}, \hat{G})$ given fixed pairs of data $\{(x_i, \tilde{x}_i)\}_{i=1}^n$, where the distance dist is defined as follows: For any matrices $A \in \mathbb{R}^{r \times d}$ and $A' \in \mathbb{R}^{r \times d}$, define the distance as

$$\text{dist}(A, A') \triangleq \min_{O \in \mathbb{O}_{r,r}} \|OA - A'\|_F.$$

Assumption B.1 (Local Directional Strong Convexity of \mathcal{L}_L). Assume that there exists some $\gamma > 0$ such that for any G satisfying $\|G - \hat{G}\|_F \leq \gamma$, the following inequalities hold for all $Z \in \mathbb{R}^{r \times d}$:

$$\text{vec}(Z)^\top \frac{\partial^2 \mathcal{L}_L(G)}{\partial \text{vec}(G) \partial \text{vec}(G)^\top} \text{vec}(Z) \leq \beta_u \|Z\|_F^2. \quad (\text{B.1})$$

$$\text{vec}(H_Z Z - \hat{G})^\top \frac{\partial^2 \mathcal{L}_L(G)}{\partial \text{vec}(G) \partial \text{vec}(G)^\top} \text{vec}(H_Z Z - \hat{G}) \geq \beta_l \|H_Z Z - \hat{G}\|_F^2, \quad (\text{B.2})$$

where $H_Z \triangleq \arg \min_{O \in \mathbb{O}_{r,r}} \|OZ - \hat{G}\|_F$.

Before presenting the theorem and its proof, we list lemmas to be used in the proof. The proofs of lemmas are deferred to Section C.

Lemma B.2. Suppose that Assumption B.1 holds with triple $(\beta_u, \beta_l, \gamma)$ and that

$$\text{dist}^2(G, \hat{G}) \leq \gamma^2. \quad (\text{B.3})$$

Let $H \triangleq \arg \min_{H \in \mathbb{O}_{r,r}} \|HG - \hat{G}\|_F$. Define $\bar{G} \triangleq G - \eta \partial_G \mathcal{L}_L(G)$ and $\tilde{G} \triangleq G - \eta g$, where $g \in \mathbb{R}^{r \times d}$ is any matrix. If $\eta \leq 1/\beta_u$, then,

$$\begin{aligned} \|H\bar{G} - \hat{G}\|_F^2 &\leq (1 - \eta\beta_l) \text{dist}^2(G, \hat{G}), \\ \|H\tilde{G} - \hat{G}\|_F^2 &\leq (1 - \eta\beta_l) \text{dist}^2(G, \hat{G}) + 2\eta \langle H\bar{G} - \hat{G}, \partial_G \mathcal{L}_L(G) - g \rangle + \eta^2 \|g - \partial_G \mathcal{L}_L(G)\|_F^2. \end{aligned}$$

Lemma B.3. Let $\mathcal{B} \subset [n]$ be a uniformly sampled random batch of size b in $[n]$. Then,

$$\mathbb{E}_{\mathcal{B}}[\partial_G \mathcal{L}_L(G; \mathcal{B})] = \partial_G \mathcal{L}_L(G)$$

holds for all $G \in \mathbb{R}^{r \times d}$, where the expectation is taken with respect to subsampling.

Define $R \triangleq (\max_{i \in [n]} \|x_i\|)(\max_{i \in [n]} \|\tilde{x}_i\|)$.

Lemma B.4. Fix $T > 0$. Suppose that $\max_{t \in [T]} \text{dist}(G^{(t)}, \hat{G})^2 \leq \gamma^2$ holds. Then,

$$\max_{t \in [T]} \|\partial_G \mathcal{L}_L(G^{(t)}; \mathcal{B}^{(t)}) - \partial_G \mathcal{L}_L(G^{(t)})\|_F \lesssim (\|\hat{G}\|_F + \gamma) R \left(\sqrt{\frac{(1 - b/n) \log(T(n + d))}{b}} + \frac{1}{b} \right)$$

holds with probability $1 - O((n + d)^{-1})$.

Lemma B.5. Suppose that x_i, \tilde{x}_i are generated according to the model in equation 5.2. Suppose that $\max_{t \in [T]} \text{dist}^2(G^{(t)}, \hat{G}) \leq \gamma^2$, where γ satisfies $\gamma \leq 1 \wedge 1/\alpha$. Then,

$$\max_{t \in [T]} \|\partial_G \mathcal{L}_L(G^{(t)}; \mathcal{B}^{(t)})\|_F \lesssim (\sqrt{r}\|\hat{G}\| + 1) R \sqrt{\frac{\log(T(n + d))}{b}} + \gamma \|\hat{\Sigma}_{x, \tilde{x}}\| + \alpha(\|\hat{G}\|^2 + 1)\gamma$$

holds with probability $1 - O((n + d)^{-1})$.

Using above lemmas, we obtain the following theorem.

Theorem B.1. Suppose that Assumption B.1 holds with triple $(\beta_u, \beta_l, \gamma)$ and that

$$\text{dist}^2(G^{(0)}, \hat{G}) \leq \frac{\gamma^2}{8}. \quad (\text{B.4})$$

We obtain a sequence of representations $(G^{(t)})_{t \in [T]}$ from noisy mini-batch SGD according to Algorithm 1 with linear loss \mathcal{L}_L . Set the clipping threshold c and the mini-batch size b as

$$c \gg (\sqrt{r}\|\hat{G}\| + 1) R \sqrt{\frac{\log(T(n + d))}{b}} + \gamma \|\hat{\Sigma}_{x, \tilde{x}}\| + \alpha(\|\hat{G}\|^2 + 1)\gamma, \quad (\text{B.5})$$

$$b \gg \frac{1}{\gamma^2} (\sqrt{r}\|\hat{G}\| + \gamma)^2 R^2 \log(T(n + d)). \quad (\text{B.6})$$

If $\eta > 0$ satisfies

$$\eta \leq \min \left\{ \frac{1}{2\beta_u}, \frac{\beta_l \gamma^2}{4\sigma^2 c^2 (2rd + 60 \log(T(n + d)))} \right\}, \quad (\text{B.7})$$

then,

$$\begin{aligned} \text{dist}^2(G^{(T)}, \hat{G}) &\lesssim (1 - \eta\beta_l)^T \text{dist}^2(G^{(0)}, \hat{G}) + \frac{\eta\sigma^2 c^2}{\beta_l} (rd + \log(T(n + d))) \\ &\quad + \frac{\eta}{\beta_l} (\sqrt{r}\|\hat{G}\| + \gamma)^2 R^2 \left(\sqrt{\frac{(1 - b/n) \log(T(n + d))}{b}} + \frac{1}{b} \right)^2. \end{aligned}$$

holds with probability $1 - O((n + d)^{-1})$.

Proof of Theorem B.1. For notational brevity, write $g^{(t)} = \partial_G \mathcal{L}_L(G^{(t)}; \mathcal{B}^{(t)})$. Define $H^{(t)} \triangleq \arg \min_{H \in \mathbb{O}_{r, r}} \|HG^{(t)} - \hat{G}\|_F$. Also define $\tilde{G}^{(t+1)} := G^{(t)} - \eta g^{(t)}$. From equation B.5 and Lemma B.5,

$$\max_{t \in [T]} \|\partial_G \mathcal{L}_L(G^{(t)}; \mathcal{B}^{(t)})\|_F \leq c$$

holds with probability $1 - O((n + d)^{-1})$. Henceforth, we focus on this event, where $h^{(t)} = 1$ holds for all $t \in [T]$. Observe that

$$\begin{aligned} \text{dist}^2(G^{(t+1)}, \hat{G}) &\leq \|H^{(t)} G^{(t+1)} - \hat{G}\|_F^2 \\ &= \|H^{(t)} \tilde{G}^{(t+1)} - \hat{G} - \eta \sigma c H^{(t)} \Gamma^{(t)}\|_F^2 \\ &= \|H^{(t)} \tilde{G}^{(t+1)} - \hat{G}\|_F^2 - 2\eta \sigma c \text{tr} \left((H^{(t)} \tilde{G}^{(t+1)} - \hat{G})^\top H^{(t)} \Gamma^{(t)} \right) + \eta^2 \sigma^2 c^2 \|\Gamma^{(t)}\|_F^2. \end{aligned} \quad (\text{B.8})$$

Define $D^{(t+1)} \triangleq \|H^{(t)}\tilde{G}^{(t+1)} - \hat{G}\|_F$. Observe that

$$\begin{aligned} -2\eta\sigma c \operatorname{tr}\left((H^{(t)}\tilde{G}^{(t+1)} - \hat{G})^\top H^{(t)}\Gamma^{(t)}\right) &= -2\eta\sigma c \sum_{j \in [r], k \in [d_1]} (H^{(t)\top}(H^{(t)}\tilde{G}^{(t+1)} - \hat{G}))_{jk}(\Gamma^{(t)})_{jk} \\ &\triangleq 2\eta\sigma c D^{(t+1)}u^{(t)}. \end{aligned}$$

Also,

$$\eta^2\sigma^2c^2\|\Gamma^{(t)}\|_F^2 = \eta^2\sigma^2c^2 \operatorname{tr}\left(\Gamma^{(t)\top}\Gamma^{(t)}\right) = \eta^2\sigma^2c^2 \sum_{j \in [r], k \in [d]} (\Gamma^{(t)})_{ij}^2 \triangleq \eta^2\sigma^2c^2v^{(t)}.$$

Since $\operatorname{vec}(\Gamma^{(t)}) \sim N(0, I_{rd})$, $u^{(t)} \sim N(0, 1)$ and $v^{(t)} \sim \chi_{rd}^2$. For simplicity, write $d^{(t)} \triangleq \operatorname{dist}(G^{(t)}, \hat{G})$. Now we have the following inequality:

$$d^{(t+1)2} \leq D^{(t+1)2} + 2\eta\sigma c D^{(t+1)}u^{(t)} + \eta^2\sigma^2c^2v^{(t)}.$$

Let $V \triangleq \max_{t \in [T]} \|g^{(t)} - \partial_G \mathcal{L}_L(G^{(t)})\|_F$. Using Lemma B.2, we obtain

$$\begin{aligned} d^{(t+1)2} &\leq (1 - \eta\beta_l)d^{(t)2} + 2\eta\langle H^{(t)}(G^{(t)} - \eta\partial_G \mathcal{L}_L(G^{(t)})) - \hat{G}, \partial_G \mathcal{L}_L(G^{(t)}) - g^{(t)} \rangle + \eta^2V^2 \\ &\quad + 2\eta\sigma c D^{(t+1)}u^{(t)} + \eta^2\sigma^2c^2v^{(t)}, \end{aligned} \tag{B.9}$$

which holds for all $t \in [T]$.

We show by induction that the following inequality holds with probability $1 - O(sT^{-1}(n+d)^{-1})$ for any fixed $s \in [T]$:

$$d^{(s)2} \leq \min\{\gamma^2, \quad 4(1 - \eta\beta_l)^s d^{(0)2} + L\}, \tag{B.10}$$

where $L > 0$ is the solution of $L - C_2\sqrt{L} - C_1^2 = 0$ with

$$\begin{aligned} C_1 &\triangleq \sqrt{\frac{\eta}{\beta_l}\sigma^2c^2(rd + 14\log^2(T(n+d))) + 7\frac{\eta}{\beta_l}V^2\log(T(n+d))}, \\ C_2 &\triangleq 2\sigma c\sqrt{2\log(T(n+d))\frac{\eta}{\beta_l}} + 2V\sqrt{\log(T(n+d))\frac{\eta}{\beta_l}}. \end{aligned}$$

Step 1. We start from $s = 1$. From a standard concentration inequality for Gaussian random variables, (see, for example, Proposition 2.5 of Wainwright (2019).)

$$u^{(0)} \leq \sqrt{2\log(T(n+d))} \tag{B.11}$$

holds with probability at least $1 - T^{-1}(n+d)^{-1}$. From a concentration bound for chi-squared distribution, (see, for example, Lemma 1 of Laurent and Massart (2000).)

$$v^{(0)} \leq rd + 2\log(T(n+d)) \tag{B.12}$$

holds with probability $1 - cT^{-1}(n+d)^{-1}$ for some universal constant $c > 0$. Note that Lemma B.2 and Cauchy-Schwarz inequality yield

$$\begin{aligned} D^{(1)2} &\leq (1 - \eta\beta_l)d^{(0)2} + 2\eta d^{(0)}V + \eta^2V^2 \\ &\leq (1 - \eta\beta_l)d^{(0)2} + \eta\beta_l d^{(0)2} + 2\frac{\eta}{\beta_l}V^2 \\ &\leq 2(1 - \eta\beta_l)d^{(0)2} + 2\frac{\eta}{\beta_l}V^2, \end{aligned}$$

where we used $2xy \leq x^2 + y^2$ in the second inequality and $\eta\beta_l \leq 1/2 \leq 1 - \eta\beta_l$ in the third inequality. Using $\sqrt{x+y} \leq \sqrt{x} + \sqrt{y}$ for $x, y \geq 0$, we further obtain

$$D^{(1)} \leq \sqrt{2}(1 - \eta\beta_l)^{1/2}d^{(0)} + \sqrt{2\frac{\eta}{\beta_l}}V.$$

Combined with equation B.9, B.11 and B.12, we have

$$\begin{aligned} d^{(1)2} &\leq D^{(1)2} + 2\eta\sigma c D^{(1)}u^{(0)} + \eta^2\sigma^2c^2v^{(0)} \\ &\leq 2(1 - \eta\beta_l)d^{(0)2} + 2\frac{\eta}{\beta_l}V^2 + 2\eta\sigma c\sqrt{2\log(T(n+d))}D^{(1)} + \eta^2\sigma^2c^2(rd + 2\log(T(n+d))) \\ &\leq 2(1 - \eta\beta_l)d^{(0)2} + 2\frac{\eta}{\beta_l}V^2 + 4\eta\sigma c\sqrt{2\log(T(n+d))}\left((1 - \eta\beta_l)^{1/2}d^{(0)} + \sqrt{\frac{\eta}{\beta_l}}V\right) \\ &\quad + \eta^2\sigma^2c^2(rd + 2\log(T(n+d))) \\ &\leq 4(1 - \eta\beta_l)d^{(0)2} + 4\frac{\eta}{\beta_l}V^2 + \eta^2\sigma^2c^2(rd + 10\log(T(n+d))), \end{aligned}$$

where we used $2xy \leq x^2 + y^2$ in the last inequality. Notice that

$$\begin{aligned} \eta^2\sigma^2c^2(rd + 10\log(T(n+d))) + 4\frac{\eta}{\beta_l}V^2 &\leq \frac{\eta\sigma^2c^2}{\beta_l}(rd + 14\log^2(T(n+d))) + 7\frac{\eta}{\beta_l}V^2\log(T(n+d)) \\ &= C_1^2 = L - C_2\sqrt{L} \leq L. \end{aligned}$$

From equation B.4, equation B.7 and $L \leq \gamma^2/2$, which will be proved later,

$$4(1 - \eta\beta_l)d^{(0)2} + \eta^2\sigma^2c^2(rd + 10\log(T(n+d))) \leq 4\frac{\gamma^2}{8} + \frac{\gamma^2}{2} \leq \gamma^2.$$

Therefore, we verify equation B.10 for $s = 1$.

Step 2. Fix $s \in [T]$. Suppose that equation B.10 holds for all t satisfying $1 \leq t \leq s-1$ on the event E . Examining the induction steps, we can show that the event E occurs with probability at least $1 - (1+c)(s-1)T^{-1}(n+d)^{-1}$. A similar concentration argument for $v^{(t)}$ gives,

$$\begin{aligned} d^{(s)2} &\leq (1 - \eta\beta_l)d^{(s-1)2} + 2\eta\langle H^{(s-1)}(G^{(s-1)} - \eta\partial_G\mathcal{L}_L(G^{(s-1)})) - \hat{G}, \partial_G\mathcal{L}_L(G^{(s-1)}) - g^{(s-1)} \rangle + \eta^2V^2 \\ &\quad + 2\eta\sigma c D^{(s)}u^{(s-1)} + \eta^2\sigma^2c^2(rd + 2\log(T(n+d))) \end{aligned} \quad (\text{B.13})$$

holds with probability at least $1 - (1+c)(s-1)T^{-1}(n+d)^{-1} - cT^{-1}(n+d)^{-1}$. Applying equation B.13 repeatedly,

$$\begin{aligned} d^{(s)2} &\leq (1 - \eta\beta_l)^s d^{(0)2} + \frac{1}{\eta\beta_l} \{ \eta^2\sigma^2c^2(rd + 2\log(T(n+d))) + \eta^2V^2 \} \\ &\quad + \underbrace{2\eta\sigma c \sum_{t'=0}^{s-1} (1 - \eta\beta_l)^{s-t'-1} D^{(t'+1)}u^{(t')}}_{T_1^{(s-1)}} \\ &\quad + \underbrace{2\eta \sum_{t'=0}^{s-1} (1 - \eta\beta_l)^{s-t'-1} \langle H^{(t')}(G^{(t')} - \eta\partial_G\mathcal{L}_L(G^{(t')})) - \hat{G}, \partial_G\mathcal{L}_L(G^{(t')}) - g^{(t')} \rangle}_{T_2^{(s-1)}}. \end{aligned} \quad (\text{B.14})$$

holds with probability at least $1 - (1+c)(s-1)T^{-1}(n+d)^{-1} - cT^{-1}(n+d)^{-1}$.

Before bounding $T_1^{(s-1)}$ and $T_2^{(s-1)}$, we derive a concentration inequality for the following sum:

$$S_a^{(t-1)} \triangleq \sum_{t'=0}^{t-1} a^{t-t'-1} \langle H^{(t')}(G^{(t')}) - \partial_G \mathcal{L}_L(G^{(t')}) - \hat{G}, \partial_G \mathcal{L}_L(G^{(t')}) - g^{(t')} \rangle,$$

where $a \in (0, 1)$. Fix $t > 0$. Let $\mathcal{F}^{(t')}$ be a filtration generated from $g^{(0)}, g^{(1)}, \dots, g^{(t')}$. Using Cauchy-Schwarz inequality and Lemma B.2, we obtain

$$|\langle H^{(t')}(G^{(t')}) - \eta \partial_G \mathcal{L}_L(G^{(t')}) - \hat{G}, \partial_G \mathcal{L}_L(G^{(t')}) - g^{(t')} \rangle| \leq (1 - \eta \beta_l) d^{(t')} V.$$

From Lemma B.3, $\mathbb{E}[g^{(t)} | \mathcal{F}^{(t-1)}] = \partial_G \mathcal{L}_L(G^{(t)})$. Since $G^{(t')}$ and $\partial_G \mathcal{L}_L(G^{(t')})$ are $\mathcal{F}^{(t'-1)}$ -measurable,

$$\mathbb{E}[\langle H^{(t')}(G^{(t')}) - \eta \partial_G \mathcal{L}_L(G^{(t')}) - \hat{G}, \partial_G \mathcal{L}_L(G^{(t')}) - g^{(t')} \rangle | \mathcal{F}^{(t'-1)}] = 0.$$

Thus $S_a^{(t-1)}$ is a sum of martingale difference sequence. Using Azuma-Hoeffding bound (See, for example, Corollary 2.20 of Wainwright (2019)), we obtain

$$|S_a^{(t-1)}| \leq \sqrt{\log(T(n+d)) \sum_{t'=0}^{t-1} a^{2t-2t'-2} (1 - \eta \beta_l) d^{(t')2} V^2}.$$

with probability $1 - O(T^{-1}(n+d)^{-1})$. By a union bound argument,

$$\max_{t \in [T]} |S_a^{(t-1)}| \leq \sqrt{\log(T(n+d)) \sum_{t'=0}^{t-1} a^{2t-2t'-2} (1 - \eta \beta_l) d^{(t')2} V^2} \quad (\text{B.15})$$

holds with probability $1 - O((n+d)^{-1})$.

Here we bound the term $T_1^{(s-1)}$, since $u_1^{(0)}, u_2^{(0)}, u_1^{(1)}, u_2^{(1)}, \dots, u_1^{(s-1)}, u_2^{(s-1)}$ are i.i.d. standard normal random variables,

$$\begin{aligned} T_1^{(s-1)} &\leq 2\eta\sigma c \sqrt{2\text{Var}(w^{(s-1)}) \log(T(n+d))} \\ &\leq 2\eta\sigma c \sqrt{\log(T(n+d)) \sum_{t'=0}^{s-1} (1 - \eta \beta_l)^{2s-2t'-2} D^{(t'+1)2}}. \end{aligned}$$

We bound $\sum_{t'=0}^{s-1} (1 - \eta \beta_l)^{2s-2t'-2} D^{(t'+1)2}$. From Lemma B.2 and equation B.10,

$$\begin{aligned} &\sum_{t'=0}^{s-1} (1 - \eta \beta_l)^{2s-2t'-2} D^{(t'+1)2} \\ &\leq \sum_{t'=0}^{s-1} (1 - \eta \beta_l)^{2s-2t'-2} \left((1 - \eta \beta_l) d^{(t')2} + 2\eta \langle H^{(t')}(G^{(t')}) - \eta \partial_G \mathcal{L}_L(G^{(t')}) - \hat{G}, \partial_G \mathcal{L}_L(G^{(t')}) - \eta g^{(t')} \rangle + \eta^2 V^2 \right) \\ &\leq \sum_{t'=0}^{s-1} 4(1 - \eta \beta_l)^{2s-t'-1} d^{(0)2} + \sum_{t'=0}^{s-1} (1 - \eta \beta_l)^{2s-2t'-1} L + 2\eta S_{(1-\eta\beta_l)^2}^{(s-1)} + \sum_{t'=0}^{s-1} (1 - \eta \beta_l)^{2s-2t'-2} \eta^2 V^2. \end{aligned}$$

Since $1 - \eta \beta_l \leq 1$,

$$\sum_{t'=0}^{s-1} (1 - \eta \beta_l)^{4s-4t'-4} \leq \sum_{t'=0}^{s-1} (1 - \eta \beta_l)^{3s-3t'-3} \leq \sum_{t'=0}^{s-1} (1 - \eta \beta_l)^{2s-2t'-2} \leq \sum_{t'=0}^{s-1} (1 - \eta \beta_l)^{s-t'-1} \leq \frac{1}{\eta \beta_l}. \quad (\text{B.16})$$

Combined with Lemma B.2, equation B.10, equation B.15 and equation B.16,

$$\begin{aligned}
& \sum_{t'=0}^{s-1} (1 - \eta\beta_l)^{2s-2t'-2} D^{(t'+1)2} \\
& \leq 4(1 - \eta\beta_l)^s \frac{1}{\eta\beta_l} d^{(0)2} + \frac{L}{\eta\beta_l} + 2\eta \sqrt{\log(T(n+d)) \sum_{t'=0}^{s-1} (1 - \eta\beta_l)^{4s-4t'-3} d^{(t')2} V^2} + \frac{\eta}{\beta_l} V^2 \\
& \leq 4(1 - \eta\beta_l)^s \frac{1}{\eta\beta_l} d^{(0)2} + \frac{L}{\eta\beta_l} + \frac{\eta}{\beta_l} V^2 + 4\eta V \sqrt{\log(T(n+d)) \sum_{t'=0}^{s-1} (1 - \eta\beta_l)^{4s-3t'-3} d^{(0)2}} \\
& \quad + 2\eta V \sqrt{\log(T(n+d)) \sum_{t'=0}^{s-1} (1 - \eta\beta_l)^{4s-4t'-3} L} \\
& = 4(1 - \eta\beta_l)^s \frac{1}{\eta\beta_l} d^{(0)2} + \frac{L}{\eta\beta_l} + \frac{\eta}{\beta_l} V^2 + 4\eta V \sqrt{\log(T(n+d)) (1 - \eta\beta_l)^s d^{(0)2} \sum_{t'=0}^{s-1} (1 - \eta\beta_l)^{3s-3t'-3}} \\
& \quad + 2\eta V \sqrt{\log(T(n+d)) \sum_{t'=0}^{s-1} (1 - \eta\beta_l)^{4s-4t'-3} L} \\
& \leq 4(1 - \eta\beta_l)^s \frac{1}{\eta\beta_l} d^{(0)2} + \frac{L}{\eta\beta_l} + \frac{\eta}{\beta_l} V^2 + 4\eta V \sqrt{\log(T(n+d)) (1 - \eta\beta_l)^s d^{(0)2} \frac{1}{\eta\beta_l}} \\
& \quad + 2\eta V \sqrt{\log(T(n+d)) L \frac{1}{\eta\beta_l}} \\
& \leq 8(1 - \eta\beta_l)^s \frac{1}{\eta\beta_l} d^{(0)2} + 2\frac{L}{\eta\beta_l} + \frac{\eta}{\beta_l} V^2 + 3\eta^2 V^2 \log(T(n+d))
\end{aligned}$$

holds with probability at least $1 - T^{-1}(n+d)^{-1}$, where we used $\sqrt{x+y} \leq \sqrt{x} + \sqrt{y}$ and $2\sqrt{xy} \leq x+y$ for $x, y \geq 0$. Therefore,

$$\begin{aligned}
T_1^{(s-1)} & \leq 2\eta\sigma c \sqrt{\log(T(n+d)) \left(8(1 - \eta\beta_l)^s \frac{1}{\eta\beta_l} d^{(0)2} + 2\frac{L}{\eta\beta_l} + \frac{\eta}{\beta_l} V^2 + 3\eta^2 V^2 \log(T(n+d)) \right)} \\
& \leq 4\eta\sigma c \sqrt{2\log(T(n+d)) (1 - \eta\beta_l)^s \frac{1}{\eta\beta_l} d^{(0)2}} + 2\eta\sigma c \sqrt{2\log(T(n+d)) \frac{L}{\eta\beta_l}} \\
& \quad + 2\eta\sigma c \sqrt{\log(T(n+d)) \frac{\eta}{\beta_l} V^2} + 2\eta\sigma c \sqrt{3\log^2(T(n+d)) \eta^2 V^2} \\
& \leq (1 - \eta\beta_l)^s d^{(0)2} + 8\sigma^2 c^2 \frac{\eta}{\beta_l} \log(T(n+d)) + 2\sigma c \sqrt{2\log(T(n+d)) \frac{\eta}{\beta_l} L} \\
& \quad + \eta^2 \sigma^2 c^2 \log(T(n+d)) + \frac{\eta}{\beta_l} V^2 + 3\eta^2 \sigma^2 c^2 \log^2(T(n+d)) + \eta^2 V^2, \tag{B.17}
\end{aligned}$$

where we used $\sqrt{x+y} \leq \sqrt{x} + \sqrt{y}$ for $x, y \geq 0$ and $2xy \leq x^2 + y^2$.

We bound the term $T_2^{(s-1)}$. Using equation B.15 and equation B.10,

$$\begin{aligned}
T_2^{(s-1)} &= 2\eta S_{1-\eta\beta_l}^{(s-1)} \\
&\leq 2\eta V \sqrt{\log(T(n+d)) \sum_{t'=0}^{s-1} (1-\eta\beta_l)^{2s-2t'-1} d^{(t')^2}} \\
&\leq 4\eta V \sqrt{\log(T(n+d)) \sum_{t'=0}^{s-1} (1-\eta\beta_l)^{2s-t'-1} d^{(0)^2}} + 2\eta V \sqrt{\log(T(n+d)) \sum_{t'=0}^{s-1} (1-\eta\beta_l)^{2s-2t'-1} L} \\
&\leq 4\eta V \sqrt{\log(T(n+d)) (1-\eta\beta_l)^s \frac{1}{\eta\beta_l} d^{(0)^2}} + 2\eta V \sqrt{\log(T(n+d)) \frac{1}{\eta\beta_l} L} \\
&= 4V \sqrt{\log(T(n+d)) (1-\eta\beta_l)^s \frac{\eta}{\beta_l} d^{(0)^2}} + 2V \sqrt{\log(T(n+d)) \frac{\eta}{\beta_l} L} \\
&\leq 4 \frac{\eta}{\beta_l} V^2 \log(T(n+d)) + 2(1-\eta\beta_l)^s d^{(0)^2} + 2V \sqrt{\log(T(n+d)) \frac{\eta}{\beta_l} L}, \tag{B.18}
\end{aligned}$$

where we used $\sqrt{x+y} \leq \sqrt{x} + \sqrt{y}$ for $x, y \geq 0$, $2xy \leq x^2 + y^2$. From equation B.14, equation B.17 and equation B.18,

$$\begin{aligned}
d^{(s)^2} &\leq (1-\eta\beta_l)^s d^{(0)^2} + \frac{1}{\eta\beta_l} \{ \eta^2 \sigma^2 c^2 (rd + 2\log(T(n+d))) + \eta^2 V^2 \} \\
&\quad + (1-\eta\beta_l)^s d^{(0)^2} + 8\sigma^2 c^2 \frac{\eta}{\beta_l} \log(T(n+d)) + 2\sigma c \sqrt{2\log(T(n+d)) \frac{\eta}{\beta_l} L} \\
&\quad + \eta^2 \sigma^2 c^2 \log(T(n+d)) + \frac{\eta}{\beta_l} V^2 + 3\eta^2 \sigma^2 c^2 \log^2(T(n+d)) + \eta^2 V^2 \\
&\quad + 4 \frac{\eta}{\beta_l} V^2 \log(T(n+d)) + 2(1-\eta\beta_l)^s d^{(0)^2} + 2V \sqrt{\log(T(n+d)) \frac{\eta}{\beta_l} L} \\
&\leq 4(1-\eta\beta_l)^s d^{(0)^2} + \frac{\eta}{\beta_l} \sigma^2 c^2 (rd + 14\log^2(T(n+d))) + 7 \frac{\eta}{\beta_l} V^2 \log(T(n+d)) \\
&\quad + \left(2\sigma c \sqrt{2\log(T(n+d)) \frac{\eta}{\beta_l}} + 2V \sqrt{\log(T(n+d)) \frac{\eta}{\beta_l}} \right) \sqrt{L}
\end{aligned}$$

holds with probability at least $1 - (1+c)(s-1)T^{-1}(n+d)^{-1} - cT^{-1}(n+d)^{-1} - T^{-1}(n+d)^{-1} = 1 - (1+c)sT^{-1}(n+d)^{-1}$, where we used $2xy \leq x^2 + y^2$ in the third inequality. Note that

$$d^{(s)^2} \leq 4(1-\eta\beta_l)^s d^{(0)^2} + L,$$

since $C_2\sqrt{L} + C_1^2 = L$. Combined with equation B.4 and $L \leq \gamma^2/2$, this further gives $d^{(s)^2} \leq \gamma^2$.

Finally, we bound L . Solving $L = C_1^2 + C_2\sqrt{L}$ gives

$$\begin{aligned}
L &= \left(\frac{C_2 + \sqrt{C_2^2 + 4C_1^2}}{2} \right)^2 \leq (C_1 + C_2)^2 \leq 2C_1^2 + 2C_2^2 \\
&= 2 \frac{\eta}{\beta_l} \sigma^2 c^2 (rd + 14\log^2(T(n+d))) + 14 \frac{\eta}{\beta_l} V^2 \log(T(n+d)) \\
&\quad + 2 \left(2\sigma c \sqrt{2\log(T(n+d)) \frac{\eta}{\beta_l}} + 2V \sqrt{\log(T(n+d)) \frac{\eta}{\beta_l}} \right)^2 \\
&\leq \frac{\eta \sigma^2 c^2}{\beta_l} (2rd + 60\log^2(T(n+d))) + 30 \frac{\eta}{\beta_l} V^2 \log(T(n+d)),
\end{aligned}$$

where we used $\eta\beta_l \leq 1/2$. Note that from equation B.6 and Lemma B.4,

$$V = \max_{t \in [T]} \|g^{(t)} - \partial_G \mathcal{L}_L(G^{(t)})\|_F \lesssim (\sqrt{r}\|\hat{G}\| + \gamma)L\sqrt{\frac{\log(T(n+d))}{b}} \ll \frac{\gamma}{\sqrt{\log(T(n+d))}}.$$

Thus

$$\frac{\eta}{\beta_l} V^2 \log(T(n+d)) \leq V^2 \log(T(n+d)) \leq \frac{\gamma^2}{4 \cdot 30}.$$

From equation B.7, we can see that $L \leq \gamma^2/2$. Finally, since $4(1 - \eta\beta_l)^s d^{(0)2} \leq 4\gamma^2/8 = \gamma^2/2$,

$$d^{(s)2} \leq \min \left\{ \gamma^2, \quad 4(1 - \eta\beta_l)^s d^{(0)2} + \frac{\eta\sigma^2 c^2}{\beta_l} (2rd + 60 \log^2(T(n+d))) + 30 \frac{\eta}{\beta_l} V^2 \right\}$$

holds with probability $1 - O(sT^{-1}(n+d)^{-1})$ for all $s \in [T]$. This concludes the induction. Again, Lemma B.4 concludes the proof. \square

B.4 Statistical Error Bound

Assumption B.2. Assume that $n \wedge d > r$ and

$$n \gg \left(\alpha^2 + \frac{1}{\alpha^2} \right) r(r + s_1^{-2} r_e(\Sigma_\xi) + s_2^{-2} r_e(\Sigma_{\bar{\xi}}))^2 \log^3(T(n+d)).$$

Assumption B.3 (Signal-to-noise Ratio). Assume that $s_1^2 \wedge s_2^2 = \Omega(1)$.

Assumption B.4 (Signal Condition Number). Assume that $\kappa \triangleq \lambda_{\max}(\Sigma_z)/\lambda_{\min}(\Sigma_z) = O(1)$.

In this section, we let $G^* = [G_1^*, G_2^*]$ be the minimizer of the loss $\mathbb{E}[\mathcal{L}_L(G)]$. Also let $\hat{G} = [\hat{G}_1, \hat{G}_2]$ be the minimizer of the loss $\mathcal{L}_L(G)$. Before going into the proof of Theorem B.1, we introduce lemmas to be used in the proof, which are based on Lemma B.7 in Gao and Ma (2021). Write $\Sigma_{x,\bar{x}} \triangleq \mathbb{E}[\hat{\Sigma}_{x,\bar{x}}]$.

Lemma B.6. Suppose that Assumption B.2 holds. Choose $\gamma > 0$ such that

$$\gamma \leq \min \left\{ 1, \quad \frac{\lambda_r(\hat{\Sigma}_{x,\bar{x}}) - \lambda_{r+1}(\hat{\Sigma}_{x,\bar{x}})}{18\alpha(1 + \lambda_1(\hat{\Sigma}_{x,\bar{x}}/\alpha)^{1/2})} \right\}. \quad (\text{B.19})$$

Then, Assumption B.1 holds with

$$\beta_u \geq 8\|\hat{\Sigma}_{x,\bar{x}}\| + 12\alpha, \quad \beta_l \leq \frac{\lambda_r(\hat{\Sigma}_{x,\bar{x}}) - \lambda_{r+1}(\hat{\Sigma}_{x,\bar{x}})}{2}.$$

Lemma B.7. Let $\mathcal{L}'_L(G; \Sigma) := -\text{tr}(G_1^\top \Sigma G_2) + (\alpha/4)\|GG^\top - I\|_F^2$. Suppose that $\lambda_r(\Sigma) > \lambda_{r+1}(\Sigma)$. Then, the minimizer $\hat{G} = [\hat{G}_1, \hat{G}_2]$ of \mathcal{L}'_L satisfies

$$\hat{G}_1 = \frac{1}{\sqrt{2}} V \left(I_r + \frac{1}{\alpha} \Lambda_{[r]} \right)^{1/2} P_{[r]}^\top, \quad \hat{G}_2 = \frac{1}{\sqrt{2}} V \left(I_r + \frac{1}{\alpha} \Lambda_{[r]} \right)^{1/2} Q_{[r]}^\top,$$

where $V \in \mathbb{O}_{r,r}$ is any orthogonal matrix, $\Lambda_{[r]}$ is the top- r singular values of Σ , and $P_{[r]}$ and $Q_{[r]}$ are the corresponding left and right singular vectors, respectively.

Theorem B.2. Suppose that Assumptions B.2, B.3 and B.4 hold. Let $G_1^{(T)}$ and $G_2^{(T)}$ be the representation obtained from algorithm 1 under the loss $\mathcal{L}_L(G)$. Suppose that initial representation $G^{(0)}$ satisfy

$$\text{dist}(G^{(0)}, \hat{G}) \ll \alpha \wedge \frac{1}{\alpha^2}. \quad (\text{B.20})$$

Choose $c \gg 1 + \alpha$ and $b = \lceil \nu n \rceil$, where $\nu \in (0, 1)$ is some constant. If $\eta > 0$ satisfies

$$\eta \ll \min \left\{ 1 + \frac{1}{\alpha}, \frac{1}{\sigma^2(\alpha^3 \vee \alpha^{-1/2})(rd + \log(T(n+d)))} \right\}, \quad (\text{B.21})$$

then,

$$\begin{aligned} & \min_{A \in \mathbb{R}^{r \times r}} \|AG_1^{(T)} - G_1^*\|_F \vee \min_{A \in \mathbb{R}^{r \times r}} \|AG_2^{(T)} - G_2^*\|_F \\ & \lesssim \left(1 - \frac{\eta}{4\kappa}\right)^{T/2} \text{dist}(G^{(0)}, \hat{G}) + \sigma(1 + \alpha)\sqrt{\eta(rd + \log(T(n+d)))} \\ & \quad + \left(1 + \frac{1}{\alpha}\right) \sqrt{\frac{r(r + s_1^{-2}r_e(\Sigma_\xi) + s_2^{-2}r_e(\Sigma_{\tilde{\xi}}))^2 \log^3(n+d)}{n}}. \end{aligned} \quad (\text{B.22})$$

holds with probability $1 - O((n+d)^{-1})$.

Corollary B.1. Assume the same conditions as in Theorem B.2. Choose η as

$$\eta = \frac{1}{\sigma\sqrt{T(rd + \log(T(n+d)))}}.$$

If T satisfies

$$T \gg \frac{1}{\sigma^2(1 + 1/\alpha)^2(rd + \log(T(n+d)))} \quad (\text{B.23})$$

$$\vee \sigma^2(\alpha^3 \vee \alpha^{-1/2})^2(rd + \log(T(n+d))), \quad (\text{B.24})$$

then

$$\begin{aligned} & \min_{A \in \mathbb{R}^{r \times r}} \|AG_1^{(T)} - G_1^*\|_F \vee \min_{A \in \mathbb{R}^{r \times r}} \|AG_2^{(T)} - G_2^*\|_F \\ & \lesssim \exp\left(-\frac{\sqrt{T}}{8\kappa\sigma\sqrt{rd + \log(T(n+d))}}\right) \text{dist}(G^{(0)}, \hat{G}) + (1 + \alpha)\sqrt{\frac{\sigma\sqrt{rd + \log(T(n+d))}}{\sqrt{T}}} \\ & \quad + \left(\alpha + \frac{1}{\alpha}\right) \sqrt{\frac{r(r + s_1^{-2}r_e(\Sigma_\xi) + s_2^{-2}r_e(\Sigma_{\tilde{\xi}}))^2 \log^3(n+d)}{n}} \end{aligned} \quad (\text{B.25})$$

holds with probability $1 - O((n+d)^{-1})$.

Proof of Corollary B.1. We directly use Theorem B.2. First, we see that condition B.21 is satisfied from the condition B.24. Note that

$$\sigma(1 + \alpha)\sqrt{\eta(rd + \log(T(n+d)))} \lesssim (1 + \alpha)\sqrt{\frac{\sigma\sqrt{rd + \log(T(n+d))}}{\sqrt{T}}}. \quad (\text{B.26})$$

The result follows from equation B.26 and equation B.22. \square

Corollary B.2 (Restatement of Theorem 5.1). Assume the same conditions as in Theorem B.2 and Corollary B.1. Choose $\sigma = C_\sigma \sqrt{T \log(1/\delta)}/(n\epsilon)$ for some universal constant C_σ . If T satisfies

$$\begin{aligned} T \gg & \left(\frac{(n\epsilon)}{(1 + 1/\alpha)\sqrt{(rd + \log(T(n+d))) \log(1/\delta)}} \right)^2 \\ & \vee \left(\frac{(\alpha^3 \vee \alpha^{-1/2})\sqrt{(rd + \log(T(n+d))) \log(1/\delta)}}{n\epsilon} \right)^2, \end{aligned}$$

then

$$\begin{aligned}
& \min_{A \in \mathbb{R}^{r \times r}} \|AG_1^{(T)} - G_1^*\|_F \vee \min_{A \in \mathbb{R}^{r \times r}} \|AG_2^{(T)} - G_2^*\|_F \\
& \lesssim \exp\left(-\frac{n\epsilon}{8\kappa C_\sigma \sqrt{\log(1/\delta)\{rd + \log(T(n+d))\}}}\right) \text{dist}(G^{(0)}, \hat{G}) + (1+\alpha) \frac{(rd + \log(T(n+d)))^{1/4} \log^{1/4}(1/\delta)}{\sqrt{n\epsilon}} \\
& + \left(\alpha + \frac{1}{\alpha}\right) \sqrt{\frac{r(r + s_1^{-2}r_e(\Sigma_\xi) + s_2^{-2}r_e(\Sigma_{\tilde{\xi}}))^2 \log^3(n+d)}{n}}
\end{aligned} \tag{B.27}$$

holds with probability $1 - O((n+d)^{-1})$.

Corollary B.2 directly follows from Corollary B.1 with the choice $\sigma \gg \sqrt{T \log(1/\delta)}/(n\epsilon)$.

Proof of Theorem B.2. From Lemma B.7, we obtain

$$\hat{G}_1 = \frac{1}{\sqrt{2}} \hat{V} \left(I_r + \frac{1}{\alpha} \hat{\Lambda}_{[r]} \right)^{1/2} \hat{P}_{[r]}^\top, \quad \hat{G}_2 = \frac{1}{\sqrt{2}} \hat{V} \left(I_r + \frac{1}{\alpha} \hat{\Lambda}_{[r]} \right)^{1/2} \hat{Q}_{[r]}^\top,$$

where $\hat{V} \in \mathbb{O}_{r,r}$ is any orthogonal matrix, $\hat{\Lambda}_{[r]} = \text{diag}(\hat{\lambda}_1, \dots, \hat{\lambda}_r)$ is the top- r singular values of $\hat{\Sigma}_{x,\tilde{x}}$, $\hat{P}_{[r]}$ and $\hat{Q}_{[r]}$ are the left and singular vectors of $\hat{\Sigma}_{x,\tilde{x}}$, respectively. Since $\mathbb{E}[\mathcal{L}_L(G)] = \mathcal{L}'_L(G; \Sigma_{x,\tilde{x}})$, we also obtain

$$G_1^* = \frac{1}{\sqrt{2}} V \left(I_r + \frac{1}{\alpha} \Lambda_{[r]} \right)^{1/2} P_{[r]}^\top, \quad G_2^* = \frac{1}{\sqrt{2}} V \left(I_r + \frac{1}{\alpha} \Lambda_{[r]} \right)^{1/2} Q_{[r]}^\top,$$

where $V \in \mathbb{O}_{r,r}$ is any orthogonal matrix, $\Lambda_{[r]} = \text{diag}(\lambda_1, \dots, \lambda_r)$ is the top- r singular values of $\Sigma_{x,\tilde{x}}$, $P_{[r]}$ and $Q_{[r]}$ are the left and singular vectors of $\Sigma_{x,\tilde{x}}$, respectively.

We first bound $\min_{A \in \mathbb{R}^{r \times r}} \|A\hat{G}_1 - G_1^*\|_F$. Let $H_P \triangleq \arg \min_{O \in \mathbb{O}_{r,r}} \|O\hat{P}_{[r]}^\top - P_{[r]}^\top\|_F$. Using Theorem 3 from Yu et al. (2015), we have

$$\begin{aligned}
\|H_P \hat{P}_{[r]}^\top - P_{[r]}^\top\|_F & \lesssim \frac{(\lambda_1 + 1)}{\lambda_r^2 - \lambda_{r+1}^2} \sqrt{\frac{r(r + s_1^{-2}r_e(\Sigma_\xi) + s_2^{-2}r_e(\Sigma_{\tilde{\xi}})) \log(n+d)}{n}} \\
& \lesssim \sqrt{\frac{r(r + s_1^{-2}r_e(\Sigma_\xi) + s_2^{-2}r_e(\Sigma_{\tilde{\xi}})) \log(n+d)}{n}},
\end{aligned} \tag{B.28}$$

where we used Assumption B.4, $\lambda_{r+1} = 0$ and $\lambda_1 = 1$. Let $A_P := V(I_r + (1/\alpha)\Lambda_{[r]})^{1/2}(I_r + (1/\alpha)\hat{\Lambda}_{[r]})^{-1/2}\hat{V}^{-1}$. Then, from Assumption B.4,

$$\|A_P\|^2 \leq \frac{1 + \lambda_1/\alpha}{1 + \hat{\lambda}_r/\alpha} \lesssim 1 \vee \kappa \lesssim 1. \tag{B.29}$$

Moreover,

$$\begin{aligned}
\|A_P \hat{G}_1 - G_1^*\|_F & = \left\| V \left(I_r + \frac{1}{\alpha} \Lambda_{[r]} \right) H_P \left(I_r + \frac{1}{\alpha} \hat{\Lambda}_{[r]} \right)^{-1/2} \hat{V}^\top \hat{G}_1 - G_1^* \right\|_F \\
& = \left\| V \left(I_r + \frac{1}{\alpha} \Lambda_{[r]} \right) (H_P \hat{P}_{[r]}^\top - P_{[r]}^\top) \right\|_F \\
& \lesssim \left(1 + \frac{1}{\alpha} \right) \sqrt{\frac{r(r + s_1^{-2}r_e(\Sigma_\xi) + s_2^{-2}r_e(\Sigma_{\tilde{\xi}})) \log(n+d)}{n}},
\end{aligned} \tag{B.30}$$

where the last inequality follows from equation B.28.

Denote the j -th largest singular value of $\Sigma_{x,\tilde{x}}$ and $\hat{\Sigma}_{x,\tilde{x}}$ by λ_j and $\hat{\lambda}_j$, respectively. Note that Lemma D.1 and Assumption B.2 gives $\|\hat{\Sigma}_{x,\tilde{x}} - \Sigma_{x,\tilde{x}}\| \ll \|\Sigma_{x,\tilde{x}}\| = 1$ with probability $1 - O((n+d)^{-1})$. In particular, $\|\hat{\Sigma}_{x,\tilde{x}}\| \leq 2\|\Sigma_{x,\tilde{x}}\| = 2$. Furthermore, from Weyl's inequality, we also have $\max_{j \in [d]} |\hat{\lambda}_j - \lambda_j| \ll (\lambda_1/\lambda_j)\lambda_j \leq \kappa\lambda_j$. Thus, Assumption B.4 gives

$$\hat{\lambda}_r - \hat{\lambda}_{r+1} \geq \lambda_r - \lambda_{r+1} - |\hat{\lambda}_r - \lambda_r| - |\hat{\lambda}_{r+1} - \lambda_{r+1}| \geq \frac{\lambda_r - \lambda_{r+1}}{2} = \frac{1}{2\kappa}.$$

Choose $\gamma > 0$ such that

$$\gamma = \frac{1}{36\kappa(\alpha \vee 1)(1 + 1/(2\alpha))^{1/2}}.$$

Then, γ satisfies the condition of Lemma B.6 with probability $1 - O((n+d)^{-1})$. Thus, on this event, Assumption B.1 holds for $\mathcal{L}_L(G)$ with

$$\beta_u \geq 8\hat{\lambda}_1 + 12\alpha, \quad \beta_l \leq \frac{\hat{\lambda}_r - \hat{\lambda}_{r+1}}{2}. \quad (\text{B.31})$$

Choose $\beta_u = 16 + 12\alpha$ and $\beta_l = (\lambda_r - \lambda_{r+1})/4 = 1/(4\kappa)$, which satisfies equation B.31 from the above arguments.

From Lemma D.3,

$$\begin{aligned} R &\lesssim \sqrt{r + s_1^{-2}r_e(\Sigma_\xi)} \sqrt{r + s_2^{-2}r_e(\Sigma_{\tilde{\xi}})} \log(n+d) \\ &\lesssim (r + s_1^{-2}r_e(\Sigma_\xi) + s_2^{-2}r_e(\Sigma_{\tilde{\xi}})) \log(n+d) \end{aligned}$$

holds with probability $1 - O((n+d)^{-1})$. Choose $b = \lceil \nu n \rceil$. Since $\|\hat{G}\|^2 \leq 1 + \|\hat{\Sigma}_{x,\tilde{x}}\|/\alpha \leq 1 + 2/\alpha$,

$$\begin{aligned} &(\sqrt{r}\|\hat{G}\| + 1)R \sqrt{\frac{\log(T(n+d))}{b}} + \gamma\|\hat{\Sigma}_{x,\tilde{x}}\| + \alpha(\|\hat{G}\|^2 + 1)\gamma \\ &\lesssim \sqrt{r\left(1 + \frac{1}{\alpha}\right)} (r + s_1^{-2}r_e(\Sigma_\xi) + s_2^{-2}r_e(\Sigma_{\tilde{\xi}})) \log(n+d) \sqrt{\frac{\log(T(n+d))}{n}} + 1 + \alpha\left(1 + \frac{1}{\alpha}\right) \\ &\lesssim \sqrt{\left(1 + \frac{1}{\alpha}\right)} \frac{\sqrt{r}(r + s_1^{-2}r_e(\Sigma_\xi) + s_2^{-2}r_e(\Sigma_{\tilde{\xi}})) \log^{3/2}(n+d)}{\sqrt{n}} + 1 + \alpha \\ &\lesssim 1 + \alpha, \end{aligned} \quad (\text{B.32})$$

where the last inequality follows from Assumption B.2. Also note that

$$\begin{aligned} &\frac{1}{\gamma^2}(\sqrt{r}\|\hat{G}\| + \gamma)^2 R^2 \log(T(n+d)) \\ &\lesssim \kappa^2(\alpha^2 \vee 1) \left(1 + \frac{1}{\alpha}\right) r \left(1 + \frac{1}{\alpha}\right) (r + s_1^{-2}r_e(\Sigma_\xi) + s_2^{-2}r_e(\Sigma_{\tilde{\xi}}))^2 \log^2(n+d) \log(T(n+d)) \\ &\lesssim \left(\alpha^2 + \frac{1}{\alpha^2}\right) r (r + s_1^{-2}r_e(\Sigma_\xi) + s_2^{-2}r_e(\Sigma_{\tilde{\xi}}))^2 \log^3(T(n+d)) \\ &\ll n, \end{aligned} \quad (\text{B.33})$$

where the last inequality follows again from Assumption B.2. Choose $c \gg 1 + \alpha$. From equation B.32, equation B.33 and $b = \lceil \nu n \rceil$, we verify that equation B.5 and equation B.6 are satisfied.

From Theorem B.1, if

$$\eta \leq \min \left\{ \frac{1}{2(16 + 12\alpha)}, \frac{\lambda_r \gamma^2}{16\sigma^2 c^2 (2rd + 60 \log(T(n+d)))} \right\},$$

then the following bound holds with probability $1 - O((n+d)^{-1})$:

$$\begin{aligned} \text{dist}^2(G^{(T)}, \hat{G}) &\lesssim (1 - \eta\beta_l)^T \text{dist}^2(G^{(0)}, \hat{G}) + \frac{\eta\sigma^2 c^2}{\beta_l} (rd + \log(T(n+d))) \\ &\quad + \frac{\eta}{\beta_l} (\sqrt{r}\|\hat{G}\| + \gamma)^2 R^2 \left(\sqrt{\frac{(1-b/n) \log(T(n+d))}{b}} + \frac{1}{b} \right)^2. \end{aligned}$$

Substituting the values of c and b with a similar argument as in equation B.32 combined with $\sqrt{x+y} \leq \sqrt{x} + \sqrt{y}$ gives

$$\begin{aligned} \text{dist}(G^{(T)}, \hat{G}) &\lesssim (1 - \eta\beta_l)^{T/2} \text{dist}(G^{(0)}, \hat{G}) + \sigma c \sqrt{\frac{\eta}{\beta_l} (rd + \log(T(n+d)))} \\ &\quad + \sqrt{\frac{\eta}{\beta_l} r \left(1 + \frac{1}{\alpha}\right)} (r + r_e(\Sigma_\xi) + r_e(\Sigma_{\tilde{\xi}})) \log(n+d) \sqrt{\frac{\log(T(n+d))}{n}} \\ &\lesssim (1 - \eta\beta_l)^{T/2} \text{dist}(G^{(0)}, \hat{G}) + (1 + \alpha) \sigma \sqrt{\frac{\eta}{\beta_l} (rd + \log(T(n+d)))} \end{aligned} \quad (\text{B.34})$$

$$+ \sqrt{\frac{\eta}{\beta_l} r \left(1 + \frac{1}{\alpha}\right)} \frac{(r + r_e(\Sigma_\xi) + r_e(\Sigma_{\tilde{\xi}})) \log^{3/2}(T(n+d))}{\sqrt{n}}. \quad (\text{B.35})$$

Finally, note that

$$\begin{aligned} \min_{A \in \mathbb{R}^{r \times r}} \|AG_1^{(T)} - G_1^*\|_F &\leq \min_{A \in \mathbb{R}^{r \times r}} \|AG_1^{(T)} - A_P \hat{G}_1\|_F + \|A_P \hat{G}_1 - G_1^*\|_F \\ &= \min_{A \in \mathbb{R}^{r \times r}} \|A_P (A_P^{-1} AG_1^{(T)} - \hat{G}_1)\|_F + \|A_P \hat{G}_1 - G_1^*\|_F \\ &\leq \|A_P\| \min_{O \in \mathbb{O}_{r,r}} \|OG_1^{(T)} - \hat{G}_1\|_F + \|A_P \hat{G}_1 - G_1^*\|_F \\ &\lesssim \text{dist}(G^{(T)}, \hat{G}) + \|A_P \hat{G}_1 - G_1^*\|_F, \end{aligned}$$

where the last inequality follows from equation B.29. Using equation B.30 and equation B.35, we obtain

$$\begin{aligned} \min_{A \in \mathbb{R}^{r \times r}} \|AG_1^{(T)} - G_1^*\|_F &\leq \min_{A \in \mathbb{R}^{r \times r}} \|AG_1^{(T)} - A_P \hat{G}_1\|_F + \|A_P \hat{G}_1 - G_1^*\|_F \\ &\lesssim (1 - \eta\beta_l)^{T/2} \text{dist}(G^{(0)}, \hat{G}) + \sigma(1 + \alpha) \sqrt{\frac{\eta}{\beta_l} (rd + \log(T(n+d)))} \\ &\quad + \sqrt{\frac{\eta}{\beta_l} r \left(1 + \frac{1}{\alpha}\right)} \frac{(r + r_e(\Sigma_\xi) + r_e(\Sigma_{\tilde{\xi}})) \log^{3/2}(T(n+d))}{\sqrt{n}} \\ &\quad + \left(1 + \frac{1}{\alpha}\right) \sqrt{\frac{r(r + s_1^{-2} r_e(\Sigma_\xi) + s_2^{-2} r_e(\Sigma_{\tilde{\xi}})) \log(n+d)}{n}} \\ &\lesssim (1 - \eta\beta_l)^{T/2} \text{dist}(G^{(0)}, \hat{G}) + \sigma(1 + \alpha) \sqrt{\frac{\eta}{\beta_l} (rd + \log(T(n+d)))} \\ &\quad + \left(1 + \frac{1}{\alpha}\right) \sqrt{\frac{r(r + s_1^{-2} r_e(\Sigma_\xi) + s_2^{-2} r_e(\Sigma_{\tilde{\xi}}))^2 \log^3(n+d)}{n}}. \end{aligned}$$

A symmetric argument for \hat{G}_2 and G_2^* gives the desired result. \square

C Proof of Lemmas

Proof of Lemma B.2. We first show the following inequality, as in the proof of Lemma 4 in Chi et al. (2019).

$$2 \left\langle H \partial_G \mathcal{L}_L(G), HG - \hat{G} \right\rangle \geq \frac{1}{\beta_u} \|\partial_G \mathcal{L}_L(G)\|_F^2 + \beta_l \|HG - \hat{G}\|_F^2. \quad (\text{C.1})$$

Note that $H \partial_G \mathcal{L}_L(G) = \partial_G \mathcal{L}_L(HG)$. Applying Taylor series expansion to $\mathcal{L}_L(\hat{G})$, we obtain

$$\mathcal{L}_L(\hat{G}) = \mathcal{L}_L(HG) - \left\langle H \partial_G \mathcal{L}_L(G), HG - \hat{G} \right\rangle + \frac{1}{2} \text{vec}(HG - \hat{G})^\top \frac{\partial^2 \mathcal{L}_L(\check{G})}{\partial \text{vec}(G) \partial \text{vec}(G)^\top} \text{vec}(HG - \hat{G}),$$

where $\check{G} \triangleq HG + \tau(\hat{G} - HG)$ with some $\tau \in [0, 1]$. We can see that

$$\|\check{G} - \hat{G}\|_F^2 = (1 - \tau) \|HG - \hat{G}\|_F^2 \leq \gamma^2.$$

From equation B.2,

$$\mathcal{L}_L(\hat{G}) \geq \mathcal{L}_L(HG) - \left\langle H \partial_G \mathcal{L}_L(G), HG - \hat{G} \right\rangle + \frac{\beta_l}{2} \|HG - \hat{G}\|_F^2. \quad (\text{C.2})$$

Furthermore, from equation B.1 and equation B.3,

$$\begin{aligned} \mathcal{L}_L(\hat{G}) - \mathcal{L}_L(HG) &\leq \mathcal{L}_L\left(HG - \frac{1}{\beta_u} \partial_G \mathcal{L}_L(HG)\right) - \mathcal{L}_L(HG) \\ &\leq -\frac{1}{\beta_u} \langle \partial_G \mathcal{L}_L(HG), \partial_G \mathcal{L}_L(HG) \rangle + \frac{\beta_u}{2} \left\| \frac{1}{\beta_u} \partial_G \mathcal{L}_L(HG) \right\|_F^2 \\ &= -\frac{1}{2\beta_u} \|\partial_G \mathcal{L}_L(HG)\|_F^2 = -\frac{1}{2\beta_u} \|\partial_G \mathcal{L}_L(G)\|_F^2, \end{aligned} \quad (\text{C.3})$$

where the second inequality follows from the characterization of smoothness (Theorem 5.8 of Beck (2017).)

From equation C.2 and equation C.3, we obtain

$$\begin{aligned} -\left\langle H \partial_G \mathcal{L}_L(G), HG - \hat{G} \right\rangle + \frac{\beta_l}{2} \|HG - \hat{G}\|_F^2 &\leq \mathcal{L}_L(\hat{G}) - \mathcal{L}_L(HG) \\ &\leq -\frac{1}{2\beta_u} \|\partial_G \mathcal{L}_L(G)\|_F^2. \end{aligned}$$

This proves equation C.1.

Next, we bound $\|H\bar{G} - \hat{G}\|_F$. Observe that

$$\begin{aligned} \|H\bar{G} - \hat{G}\|_F^2 &= \|HG - \hat{G} - \eta H \partial_G \mathcal{L}_L(G)\|_F^2 \\ &= \text{dist}^2(G, \hat{G}) + \eta^2 \|\partial_G \mathcal{L}_L(G)\|_F^2 - 2\eta \left\langle \partial_G \mathcal{L}_L(G), HG - \hat{G} \right\rangle \\ &\leq (1 - \eta\beta_l) \text{dist}^2(G, \hat{G}) + \eta \left(\eta - \frac{1}{\beta_u} \right) \|\partial_G \mathcal{L}_L(G)\|_F^2 \\ &\leq (1 - \eta\beta_l) \text{dist}^2(G, \hat{G}), \end{aligned} \quad (\text{C.4})$$

where the last inequality follows from $\eta \leq 1/\beta_u$.

Using equation C.4, we further obtain

$$\begin{aligned} \|H\tilde{G} - \hat{G}\|_F^2 &= \|H\bar{G} - \hat{G} + \eta H(\partial_G \mathcal{L}_L(G) - g)\|_F^2 \\ &= \|H\bar{G} - \hat{G}\|_F^2 + 2\eta \langle H\bar{G} - \hat{G}, \partial_G \mathcal{L}_L(G) - g \rangle + \eta^2 \|g - \partial_G \mathcal{L}_L(G)\|_F^2 \\ &\leq (1 - \eta\beta_l) \text{dist}^2(G, \hat{G}) + 2\eta \langle H\bar{G} - \hat{G}, \partial_G \mathcal{L}_L(G) - g \rangle + \eta^2 \|g - \partial_G \mathcal{L}_L(G)\|_F^2. \end{aligned}$$

This concludes the proof. \square

Proof of Lemma B.3. Observe that

$$\begin{aligned}
\mathbb{E}_{\mathcal{B}} \left[\frac{1}{b} \sum_{i \in \mathcal{B}} x_i \tilde{x}_i^\top \right] &= \frac{1}{b} \frac{1}{\binom{n}{b}} \sum_{\substack{\mathcal{B}' \subset [n] \\ |\mathcal{B}'|=b}} \sum_{i \in \mathcal{B}'} x_i \tilde{x}_i^\top \\
&= \frac{1}{b} \frac{1}{\binom{n}{b}} \sum_{i \in [n]} x_i \tilde{x}_i^\top \sum_{\substack{\mathcal{B}' \subset [n] \\ |\mathcal{B}'|=b}} \mathbf{1}\{i \in \mathcal{B}'\} \\
&= \frac{1}{b} \frac{\binom{n-1}{b-1}}{\binom{n}{b}} \sum_{i \in [n]} x_i \tilde{x}_i^\top \\
&= \frac{1}{n} \sum_{i \in [n]} x_i \tilde{x}_i^\top.
\end{aligned}$$

Similarly,

$$\begin{aligned}
\mathbb{E}_{\mathcal{B}} \left[\frac{1}{b(b-1)} \sum_{\substack{i,j \in \mathcal{B} \\ i \neq j}} x_i \tilde{x}_j^\top \right] &= \frac{1}{b(b-1)} \frac{1}{\binom{n}{b}} \sum_{\substack{\mathcal{B}' \subset [n] \\ |\mathcal{B}'|=b}} \sum_{\substack{i,j \in \mathcal{B}' \\ i \neq j}} x_i \tilde{x}_j^\top \\
&= \frac{1}{b(b-1)} \frac{\binom{n-2}{b-2}}{\binom{n}{b}} \sum_{\substack{i,j \in [n] \\ i \neq j}} x_i \tilde{x}_j^\top \\
&= \frac{1}{n(n-1)} \sum_{\substack{i,j \in [n] \\ i \neq j}} x_i \tilde{x}_j^\top.
\end{aligned}$$

Thus $\mathbb{E}_{\mathcal{B}}[\hat{\Sigma}_{x,\tilde{x},\mathcal{B}}] = \mathbb{E}_{\mathcal{B}}[\hat{\Sigma}_{x,\tilde{x}}]$ and hence

$$\mathbb{E}_{\mathcal{B}}[\mathcal{L}_L(G; \mathcal{B})] = \mathcal{L}_L(G). \quad (\text{C.5})$$

Taking derivative with G in equation C.5 concludes the proof. \square

Proof of Lemma B.4. Note that $\partial_G \mathcal{L}_L(G^{(t)}; \mathcal{B}^{(t)}) - \partial_G \mathcal{L}_L(G^{(t)}; \mathcal{B}^{(t)}) = \partial_G(-\text{tr}(G_1^{(t)} \hat{\Sigma}_{x,\tilde{x}} G_2^{(t)}) + \text{tr}(G_1^{(t)} \hat{\Sigma}_{x,\tilde{x},\mathcal{B}^{(t)}} G_2^{(t)}))$. Thus

$$\begin{aligned}
&\|\partial_G \mathcal{L}_L(G^{(t)}; \mathcal{B}^{(t)}) - \partial_G \mathcal{L}_L(G^{(t)}; \mathcal{B}^{(t)})\|_F \\
&= \|G_1^{(t)}(\hat{\Sigma}_{x,\tilde{x}} - \hat{\Sigma}_{x,\tilde{x},\mathcal{B}^{(t)}})\|_F + \|G_2^{(t)}(\hat{\Sigma}_{x,\tilde{x}} - \hat{\Sigma}_{x,\tilde{x},\mathcal{B}^{(t)}})^\top\|_F \\
&\leq (\|G_1^{(t)}\|_F + \|G_2^{(t)}\|_F) \|\hat{\Sigma}_{x,\tilde{x}} - \hat{\Sigma}_{x,\tilde{x},\mathcal{B}^{(t)}}\| \\
&\leq (\|\hat{G}\|_F + \text{dist}(G^{(t)}, \hat{G})) \|\hat{\Sigma}_{x,\tilde{x}} - \hat{\Sigma}_{x,\tilde{x},\mathcal{B}^{(t)}}\| \\
&\leq (\|\hat{G}\|_F + \gamma) \|\hat{\Sigma}_{x,\tilde{x}} - \hat{\Sigma}_{x,\tilde{x},\mathcal{B}^{(t)}}\|.
\end{aligned}$$

We first bound $\|(1/b) \sum_{i \in \mathcal{B}^{(t)}} x_i \tilde{x}_i^\top - (1/n) \sum_{i \in [n]} x_i \tilde{x}_i^\top\|$. Write $x_i = (x_{i1}, \dots, x_{id_1})$ and $\tilde{x}_i = (\tilde{x}_{i1}, \dots, \tilde{x}_{id_2})$. For any fixed $k \in [d_1]$ and $\ell \in [d_2]$, using Lemma D.2, we have

$$\begin{aligned}
\left| \frac{1}{b} \sum_{i \in \mathcal{B}^{(t)}} x_{ik} \tilde{x}_{i\ell} - \frac{1}{n} \sum_{i \in [n]} x_{ik} \tilde{x}_{i\ell} \right| &\leq C \max_{i \in [n]} |x_{ik} \tilde{x}_{i\ell}| \sqrt{\frac{(1-b/n) \log(Trd(n+d))}{b}} \\
&\leq CR \sqrt{\frac{(1-b/n) \log(T(n+d))}{b}}
\end{aligned}$$

with probability $1 - O(T^{-1}(rd)^{-1}(n+d)^{-1})$, where $C > 0$ is a universal constant. Note that operator norm of a matrix is bounded by the maximum element of the matrix. By a union bound argument,

$$\begin{aligned} \left\| \frac{1}{b} \sum_{i \in \mathcal{B}^{(t)}} x_i \tilde{x}_i^\top - \frac{1}{n} \sum_{i \in [n]} x_i \tilde{x}_i^\top \right\| &\leq \max_{k \in [d_1], l \in [d_2]} \left| \frac{1}{b} \sum_{i \in \mathcal{B}^{(t)}} x_{ik} \tilde{x}_{il} - \frac{1}{n} \sum_{i \in [n]} x_{ik} \tilde{x}_{il} \right| \\ &\leq CR \sqrt{\frac{(1-b/n) \log(Trd(n+d))}{b}} \end{aligned}$$

holds with probability $1 - O(T^{-1}(n+d)^{-1})$.

Let $\mu_{\mathcal{B}^{(t)}} \triangleq (1/b) \sum_{i \in \mathcal{B}^{(t)}} x_i$ and $\tilde{\mu}_{\mathcal{B}^{(t)}} \triangleq (1/b) \sum_{i \in \mathcal{B}^{(t)}} \tilde{x}_i$. Also let $\mu \triangleq (1/n) \sum_{i \in [n]} x_i$ and $\tilde{\mu} \triangleq (1/n) \sum_{i \in [n]} \tilde{x}_i$. Next we bound $\|\mu_{\mathcal{B}^{(t)}} \tilde{\mu}_{\mathcal{B}^{(t)}}^\top - \mu \tilde{\mu}^\top\|$.

Again from Lemma D.2, for any fixed $j \in [d_1]$,

$$|e_j^\top (\mu_{\mathcal{B}^{(t)}} - \mu)| \leq C' \max_{i \in [n]} |e_j^\top x_i| \sqrt{\frac{(1-b/n) \log(Td_1(n+d))}{b}}$$

holds with probability $1 - O(T^{-1}d_1^{-1}(n+d)^{-1})$, where $C' > 0$ is some universal constant. By a union bound argument, we obtain

$$\|\mu_{\mathcal{B}^{(t)}} - \mu\| \leq C' \max_{i \in [n]} \|x_i\| \sqrt{\frac{(1-b/n) \log(T(n+d))}{b}}$$

holds with probability $1 - O(T^{-1}(n+d)^{-1})$. Similarly,

$$\|\tilde{\mu}_{\mathcal{B}^{(t)}} - \tilde{\mu}\| \leq C' \max_{i \in [n]} \|\tilde{x}_i\| \sqrt{\frac{(1-b/n) \log(n+d)}{b}}$$

holds with probability $1 - O((n+d)^{-1})$. Thus,

$$\begin{aligned} \|\mu_{\mathcal{B}^{(t)}} \tilde{\mu}_{\mathcal{B}^{(t)}}^\top - \mu \tilde{\mu}^\top\| &\leq \|\mu - \mu_{\mathcal{B}^{(t)}}\| \|\tilde{\mu}_{\mathcal{B}^{(t)}}\| + \|\mu\| \|\tilde{\mu} - \tilde{\mu}_{\mathcal{B}^{(t)}}\| \\ &\leq 2C' (\max_{i \in [n]} \|x_i\|) (\max_{i \in [n]} \|\tilde{x}_i\|) \sqrt{\frac{(1-b/n) \log(T(n+d))}{b}}, \end{aligned}$$

where we used $\|\tilde{\mu}_{\mathcal{B}^{(t)}}\| \leq \max_{i \in [n]} \|\tilde{x}_i\|$ and $\|\mu\| \leq \max_{i \in [n]} \|x_i\|$. Therefore,

$$\begin{aligned} \|\hat{\Sigma}_{x, \tilde{x}, \mathcal{B}^{(t)}} - \hat{\Sigma}_{x, \tilde{x}}\| &= \left\| \frac{1}{b-1} \sum_{i \in \mathcal{B}^{(t)}} x_i \tilde{x}_i^\top - \frac{1}{n-1} \sum_{i \in [n]} x_i \tilde{x}_i^\top - \frac{b}{b-1} \mu_{\mathcal{B}^{(t)}} \tilde{\mu}_{\mathcal{B}^{(t)}}^\top + \frac{n}{n-1} \mu \tilde{\mu}^\top \right\| \\ &\leq \left\| \frac{1}{b} \sum_{i \in \mathcal{B}^{(t)}} x_i \tilde{x}_i^\top - \frac{1}{n} \sum_{i \in [n]} x_i \tilde{x}_i^\top \right\| + \|\mu_{\mathcal{B}^{(t)}} \tilde{\mu}_{\mathcal{B}^{(t)}}^\top - \mu \tilde{\mu}^\top\| \\ &\quad + \left\| \frac{1}{b} \sum_{i \in \mathcal{B}^{(t)}} x_i \tilde{x}_i^\top - \frac{1}{b-1} \sum_{i \in \mathcal{B}^{(t)}} x_i \tilde{x}_i^\top \right\| + \left\| \frac{1}{n} \sum_{i \in [n]} x_i \tilde{x}_i^\top + \frac{1}{n-1} \sum_{i \in [n]} x_i \tilde{x}_i^\top \right\| \\ &\leq (C + 2C') R \sqrt{\frac{(1-b/n) \log(T(n+d))}{b}} \\ &\quad + \frac{1}{b-1} \max_{i \in \mathcal{B}^{(t)}} \|x_i\| \|\tilde{x}_i\| + \frac{1}{n-1} \max_{i \in [n]} \|x_i\| \|\tilde{x}_i\| \\ &\leq (C + 2C' + 4) R \left(\sqrt{\frac{(1-b/n) \log(T(n+d))}{b}} + \frac{1}{b} \right) \end{aligned}$$

holds with probability $1 - O(T^{-1}(n+d)^{-1})$. A union bound argument for $t \in [T]$ concludes the proof. \square

Proof of Lemma B.5. Note that

$$\begin{aligned} \max_{t \in [T]} \|\partial_G \mathcal{L}_L(G^{(t)}; \mathcal{B})\|_F &= \max_{t \in [T]} \|\partial_G \mathcal{L}_L(G^{(t)}; \mathcal{B}) - \partial_G \mathcal{L}_L(\hat{G})\|_F \\ &\leq \max_{t \in [T]} \underbrace{\|\partial_G \mathcal{L}_L(G^{(t)}; \mathcal{B}) - \partial_G \mathcal{L}_L(G^{(t)})\|_F}_{=: T_1^{(t)}} + \max_{t \in [T]} \underbrace{\|\partial_G \mathcal{L}_L(G^{(t)}) - \partial_G \mathcal{L}_L(\hat{G})\|_F}_{=: T_2^{(t)}}. \end{aligned}$$

We can bound the term $T_1^{(t)}$ by Lemma B.4 as

$$\max_{t \in [T]} T_1^{(t)} \lesssim (\sqrt{r} \|\hat{G}\| + \gamma) R \sqrt{\frac{\log(T(n+d))}{b}}, \quad (\text{C.6})$$

which holds with probability $1 - O((n+d)^{-1})$. For the term T_2 , by triangle inequality and the inequality $\|AB\|_F \leq \|A\| \|B\|_F$ for any matrices A and B , we obtain

$$\begin{aligned} T_2^{(t)} &\leq \|(G_2^{(t)} - \hat{G}_2) \hat{\Sigma}_{x, \tilde{x}}^\top\|_F + \|(G_1^{(t)} - \hat{G}_1) \hat{\Sigma}_{x, \tilde{x}}\|_F + \alpha \|G^{(t)} G^{(t)\top} G^{(t)} - \hat{G} \hat{G}^\top \hat{G}\|_F + \alpha \|G^{(t)} - \hat{G}\|_F \\ &\leq \|G^{(t)} - \hat{G}\|_F \|\hat{\Sigma}_{x, \tilde{x}}\| + 3\alpha (\|G^{(t)}\| \vee \|\hat{G}\|)^2 \|G^{(t)} - \hat{G}\|_F \\ &\lesssim \gamma \|\hat{\Sigma}_{x, \tilde{x}}\| + \alpha (\|\hat{G}\|^2 + \gamma^2) \gamma, \end{aligned} \quad (\text{C.7})$$

where we used $\|G^{(t)}\| \leq \|\hat{G}\| + \gamma$. The claim follows from equation C.6 and equation C.7. \square

Proof of Lemma B.6. The following proof uses the technique from the proof of Lemma B.7 in Gao and Ma (2021). We first derive the bound for the smoothness of \mathcal{L}_L . To this aim, compute the derivatives of \mathcal{L}_L . For notational brevity, we write Σ for $\hat{\Sigma}_{x, \tilde{x}}$. Observe that

$$\frac{\partial}{\partial G} \|GG^\top - I_r\|_F^2 = 4GG^\top G - 4G.$$

This implies

$$\frac{\partial}{\partial \text{vec}(G)} \|GG^\top - I_r\|_F^2 = \text{vec}(4GG^\top G - 4G) = 4(I_d \otimes GG^\top) \text{vec}(G) - 4 \text{vec}(G). \quad (\text{C.8})$$

Write column vectors of G as $G = [a_1, \dots, a_d] \in \mathbb{R}^{r \times d}$. Define

$$A \triangleq \begin{pmatrix} a_1 a_1^\top & a_2 a_1^\top & \dots & a_d a_1^\top \\ a_1 a_2^\top & a_2 a_2^\top & \dots & a_d a_2^\top \\ \vdots & \vdots & \ddots & \vdots \\ a_1 a_d^\top & a_2 a_d^\top & \dots & a_d a_d^\top \end{pmatrix}.$$

Thus,

$$\frac{\partial \mathcal{L}_L(G)}{\partial G} = -G \begin{pmatrix} O & \Sigma \\ \Sigma^\top & O \end{pmatrix} + \alpha GG^\top G - \alpha G. \quad (\text{C.9})$$

Also, equation C.8 further gives

$$\frac{\partial^2}{\partial \text{vec}(G) \partial \text{vec}(G)^\top} \|GG^\top - I_r\|_F^2 = 4(I_d \otimes GG^\top) + 4G^\top G \otimes I_r + 4A - 4I_{rd}.$$

Therefore,

$$\frac{\partial^2 \mathcal{L}_L(G)}{\partial \text{vec}(G) \partial \text{vec}(G)^\top} = - \begin{pmatrix} O & \Sigma \\ \Sigma^\top & O \end{pmatrix} \otimes I_r + \alpha I_d \otimes GG^\top + \alpha G^\top G \otimes I_r + \alpha A - \alpha I_{rd}.$$

From Lemma B.7, $\hat{G} = [\hat{G}_1, \hat{G}_2]$ is given by

$$\hat{G}_1 = \frac{1}{\sqrt{2}} V \left(I_r + \frac{1}{\alpha} \Lambda_{[r]} \right)^{1/2} P_{[r]}^\top, \quad \hat{G}_2 = \frac{1}{\sqrt{2}} V \left(I_r + \frac{1}{\alpha} \Lambda_{[r]} \right)^{1/2} Q_{[r]}^\top,$$

where $V \in \mathbb{O}_{r,r}$ is any orthogonal matrix, $P_{[r]}$ and $Q_{[r]}$ are the top- r right and left singular vectors, respectively, and $\Lambda_{[r]}$ is a diagonal matrix of top- r singular values. We note that $\|\hat{G}\|^2 \leq \|\hat{G}_1\|^2 + \|\hat{G}_2\|^2 = (1 + \|\Sigma\|/\alpha)$.

Fix any $Z_1 \in \mathbb{R}^{r \times d_1}$ and $Z_2 \in \mathbb{R}^{r \times d_2}$. Let $Z = [Z_1, Z_2] \in \mathbb{R}^{r \times d}$. Write $z_1 \triangleq \text{vec}(Z_1)$, $z_2 \triangleq \text{vec}(Z_2)$ and $z = \text{vec}(Z)$. Since

$$\begin{aligned} z^\top \left(\begin{pmatrix} O & \Sigma \\ \Sigma^\top & O \end{pmatrix} \otimes I_r \right) z &= 2z_1^\top (\Sigma \otimes I_r) z_2 = 2 \text{tr}(Z_1^\top Z_2 \Sigma^\top), \\ z^\top (I_d \otimes G G^\top) z &= \text{tr}(Z^\top G G^\top Z), \\ z^\top (G^\top G \otimes I_r) z &= \text{tr}(Z^\top Z G^\top G), \\ z^\top A z &= \sum_{i,j} a_j^\top z_i a_i^\top z_j = \text{tr}(Z G^\top Z G^\top), \end{aligned}$$

we obtain

$$\begin{aligned} z^\top \frac{\partial^2 \mathcal{L}_L(G)}{\partial \text{vec}(G) \partial \text{vec}(G)^\top} z &= -2 \text{tr}(Z_1^\top Z_2 \Sigma^\top) - \alpha \text{tr}(Z^\top Z) \\ &\quad + \alpha \text{tr}(Z G^\top Z G^\top) + \alpha \text{tr}(Z^\top G G^\top Z) + \alpha \text{tr}(Z^\top Z G^\top G). \end{aligned} \quad (\text{C.10})$$

Now suppose that $\|G - \hat{G}\|_F \leq \gamma$. By Cauchy-Schwarz inequality,

$$\begin{aligned} z^\top \frac{\partial^2 \mathcal{L}_L(G)}{\partial \text{vec}(G) \partial \text{vec}(G)^\top} z &\leq 2\|Z_1\|_F \|Z_2\|_F \|\Sigma\| + 3\alpha \|Z\|_F^2 \|G\|^2 \\ &\leq (2\|\Sigma\| + 3\alpha \|G\|^2) \|Z\|_F^2. \end{aligned}$$

From $\|G\|^2 \leq (\|\hat{G}\| + \gamma)^2 \leq 2\|\hat{G}\|^2 + 2\gamma^2$, $\gamma^2 \leq 1$ and $\|\hat{G}\|^2 \leq (1 + \|\Sigma\|/\alpha)$,

$$z^\top \frac{\partial^2 \mathcal{L}_L(G)}{\partial \text{vec}(G) \partial \text{vec}(G)^\top} z \leq (8\|\Sigma\| + 12\alpha) \|Z\|_F^2. \quad (\text{C.11})$$

Setting $\beta_u \triangleq 8\|\Sigma\| + 12\alpha$ gives the first result for the smoothness of \mathcal{L}_L .

Next we derive the strong directional convexity of \mathcal{L}_L . Let $\Delta_1 \triangleq H Z_1 - \hat{G}_1$, $\Delta_2 \triangleq H Z_2 - \hat{G}_2$ and $\Delta \triangleq [\Delta_1, \Delta_2] = H Z - \hat{G}$. We bound $\text{vec}(\Delta)^\top \partial^2 \mathcal{L}_L(G) \text{vec}(\Delta)$ from below. We first deal with the case where $G = \hat{G}$. Since $\hat{G} \hat{G}^\top = (1/\alpha) V \Lambda_{[r]} V^\top + I_r$, equation C.10 gives,

$$\begin{aligned} &\text{vec}(\Delta)^\top \frac{\partial^2 \mathcal{L}_L(\hat{G})}{\partial \text{vec}(G) \partial \text{vec}(G)^\top} \text{vec}(\Delta) \\ &= -2 \text{tr}(\Delta_1^\top \Delta_2 \Sigma^\top) - \alpha \text{tr}(\Delta^\top \Delta) \\ &\quad + \alpha \text{tr}(\Delta \hat{G}^\top \Delta \hat{G}^\top) + \alpha \text{tr}(\Delta^\top \hat{G} \hat{G}^\top \Delta) + \alpha \text{tr}(\Delta^\top \Delta \hat{G}^\top \hat{G}) \\ &= \underbrace{\text{tr}(\Delta^\top V \Lambda_{[r]} V^\top \Delta)}_{=:T_1} + \underbrace{\alpha \text{tr}(\Delta^\top \Delta \hat{G}^\top \hat{G}) - 2 \text{tr}(\Delta_1^\top \Delta_2 \Sigma^\top) + \alpha \text{tr}(\Delta \hat{G}^\top \Delta \hat{G}^\top)}_{=:T_2}. \end{aligned}$$

We first bound the term T_1 . Note

$$\hat{G}^\top \hat{G} = \frac{1}{2} \begin{pmatrix} P_{[r]} \\ Q_{[r]} \end{pmatrix} \begin{pmatrix} P_{[r]} \\ Q_{[r]} \end{pmatrix}^\top + \frac{1}{2\alpha} \begin{pmatrix} P_{[r]} \Lambda_{[r]} P_{[r]}^\top & P_{[r]} \Lambda_{[r]} Q_{[r]}^\top \\ Q_{[r]} \Lambda_{[r]} P_{[r]}^\top & Q_{[r]} \Lambda_{[r]} Q_{[r]}^\top \end{pmatrix}. \quad (\text{C.12})$$

Notice that the first term is positive semi-definite. Hence,

$$\begin{aligned}\alpha \operatorname{tr}(\Delta^\top \Delta \hat{G}^\top \hat{G}) &\geq \frac{1}{2} \operatorname{tr}(\Delta_1^\top \Delta_1 P_{[r]} \Lambda_{[r]} P_{[r]}^\top) + \operatorname{tr}(\Delta_1^\top \Delta_2 Q_{[r]} \Lambda_{[r]} P_{[r]}^\top) + \frac{1}{2} \operatorname{tr}(\Delta_2^\top \Delta_2 Q_{[r]} \Lambda_{[r]} Q_{[r]}^\top) \\ &\geq 2 \operatorname{tr}(\Delta_1^\top \Delta_2 Q_{[r]} \Lambda_{[r]} P_{[r]}^\top),\end{aligned}$$

where we used $\operatorname{tr}(AB) \leq \|A\|_F \|B\|_F \leq (1/2) \operatorname{tr}(A^\top A) + (1/2) \operatorname{tr}(B^\top B)$, which follows from Cauchy-Schwarz inequality and $2xy \leq x^2 + y^2$. Let the SVD of Σ be $\Sigma = P_{[r]} \Lambda_{[r]} Q_{[r]}^\top + P_\perp \Lambda_\perp Q_\perp^\top$, where P_\perp, Q_\perp are the right and left singular vectors except top- r singular vectors, respectively, and Λ_\perp is a diagonal matrix of remaining singular values. Observe that

$$\begin{aligned}\alpha \operatorname{tr}(\Delta^\top \Delta \hat{G}^\top \hat{G}) - 2 \operatorname{tr}(\Delta_1^\top \Delta_2 \Sigma^\top) \\ \geq 2 \operatorname{tr}(\Delta_1^\top \Delta_2 Q_{[r]} \Lambda_{[r]} P_{[r]}^\top) - 2 \operatorname{tr}(\Delta_1^\top \Delta_2 Q_{[r]} \Lambda_{[r]} P_{[r]}^\top) - 2 \operatorname{tr}(\Delta_1^\top \Delta_2 Q_\perp \Lambda_\perp P_\perp^\top) \\ = -2 \operatorname{tr}(\Delta_1^\top \Delta_2 Q_\perp \Lambda_\perp P_\perp^\top).\end{aligned}$$

Thus,

$$\begin{aligned}T_1 &\geq \operatorname{tr}(\Delta^\top V \Lambda_{[r]} V^\top \Delta) - 2 \operatorname{tr}(\Delta_1^\top \Delta_2 Q_\perp \Lambda_\perp P_\perp^\top) \\ &\geq \lambda_r \|\Delta\|_F^2 - \operatorname{tr}(\Delta_2 Q_\perp \Lambda_\perp Q_\perp^\top \Delta_2^\top) - \operatorname{tr}(\Delta_1 P_\perp \Lambda_\perp P_\perp^\top \Delta_1^\top) \\ &\geq (\lambda_r - \lambda_{r+1}) \|\Delta\|_F^2,\end{aligned}$$

where we used $\operatorname{tr}(AB) \leq (1/2) \operatorname{tr}(A^\top A) + (1/2) \operatorname{tr}(B^\top B)$ again.

Next, we show $T_2 \geq 0$. Suppose that $HZ\hat{G}^\top$ is symmetric. Then,

$$\begin{aligned}\operatorname{tr}(\Delta \hat{G}^\top \Delta \hat{G}^\top) &= \operatorname{tr}((HZ - \hat{G}) \hat{G}^\top (HZ - \hat{G}) \hat{G}^\top) \\ &= \operatorname{tr}(HZ \hat{G}^\top HZ \hat{G}^\top) - 2 \operatorname{tr}(\hat{G} \hat{G}^\top HZ \hat{G}^\top) + \operatorname{tr}(\hat{G} \hat{G}^\top \hat{G} \hat{G}^\top) \\ &= \operatorname{tr}((HZ \hat{G}^\top - \hat{G} \hat{G}^\top)^\top (HZ \hat{G}^\top - \hat{G} \hat{G}^\top)) \geq 0.\end{aligned}$$

Thus, we only need to show that $HZ\hat{G}^\top$ is symmetric. Recall that $H \triangleq \arg \min_{O \in \mathbb{O}_{r,r}} \|OZ - \hat{G}\|_F^2$. This gives

$$\|HZ - \hat{G}\|_F^2 \leq \|H'Z - \hat{G}\|_F^2 \quad (\text{C.13})$$

for all $H' \in \mathbb{O}_{r,r}$. Let the SVD of $Z\hat{G}^\top$ be $Z\hat{G}^\top = UCV^\top$, where $U, V \in \mathbb{O}_{r,r'}$ are positive definite matrices and $C \in \mathbb{R}^{r'}$ is a diagonal matrix. Write the orthogonal matrices of U and V as $U_\perp \in \mathbb{O}_{r,r-r'}$ and $V_\perp \in \mathbb{O}_{r,r-r'}$, respectively. From equation C.13,

$$\operatorname{tr}(V^\top H' U C) = \sum_{j \in [r']} (V^\top H' U)_{j,j} (C)_{j,j} \leq \operatorname{tr}(V^\top H U C) \quad \forall H' \in \mathbb{O}_{r,r}. \quad (\text{C.14})$$

The inequality in equation C.14 holds if and only if $V^\top H U = I_r$. Now we decompose HU as $HU = VV^\top HU + V_\perp V_\perp^\top HU = V + V_\perp V_\perp^\top HU$. The fact that $V, HU \in \mathbb{O}_{r,r'}$ yields $HU = V$. Thus $HZ\hat{G}^\top = HUCV^\top = VCV^\top$ and hence $HZ\hat{G}^\top$ is symmetric.

In summary, we showed that

$$\operatorname{vec}(\Delta)^\top \frac{\partial^2 \mathcal{L}_L(\hat{G})}{\partial \operatorname{vec}(G) \partial \operatorname{vec}(G)^\top} \operatorname{vec}(\Delta) \geq (\lambda_r(\Sigma) - \lambda_{r+1}(\Sigma)) \|\Delta\|_F^2. \quad (\text{C.15})$$

Next, we prove that $\text{vec}(\Delta)^\top \partial^2 \mathcal{L}_L(G) \text{vec}(\Delta)$ is close to $\text{vec}(\Delta)^\top \partial^2 \mathcal{L}_L(\hat{G}) \text{vec}(\Delta)$ under assumption $\|G - \hat{G}\|_F \leq \gamma$. Observe that

$$\begin{aligned} & \text{vec}(\Delta)^\top \frac{\partial^2 \mathcal{L}_L(G)}{\partial \text{vec}(G) \partial \text{vec}(G)^\top} \text{vec}(\Delta) - \text{vec}(\Delta)^\top \frac{\partial^2 \mathcal{L}_L(\hat{G})}{\partial \text{vec}(G) \partial \text{vec}(G)^\top} \text{vec}(\Delta) \\ &= \alpha \text{tr}(\Delta G^\top \Delta G^\top) + \alpha \text{tr}(\Delta^\top G G^\top \Delta) + \alpha \text{tr}(\Delta^\top \Delta G^\top G) \\ &\quad - \alpha \text{tr}(\Delta \hat{G}^\top \Delta \hat{G}^\top) - \alpha \text{tr}(\Delta^\top \hat{G} \hat{G}^\top \Delta) - \alpha \text{tr}(\Delta^\top \Delta \hat{G}^\top \hat{G}). \end{aligned}$$

Using triangle inequality multiple times, we obtain

$$\begin{aligned} & \left| \text{vec}(\Delta)^\top \frac{\partial^2 \mathcal{L}_L(G)}{\partial \text{vec}(G) \partial \text{vec}(G)^\top} \text{vec}(\Delta) - \text{vec}(\Delta)^\top \frac{\partial^2 \mathcal{L}_L(\hat{G})}{\partial \text{vec}(G) \partial \text{vec}(G)^\top} \text{vec}(\Delta) \right| \\ & \leq 3\alpha \|\Delta\|_F^2 \|G - \hat{G}\|_F (\|G\| + \|\hat{G}\|) \\ & \leq 3\alpha \|\Delta\|_F^2 \|G - \hat{G}\|_F (\|G - \hat{G}\| + 2\|\hat{G}\|) \\ & \leq 3\alpha \|\Delta\|_F^2 \gamma \left(1 + 2 \left(1 + \frac{\|\Sigma\|}{\alpha} \right)^{1/2} \right) \\ & \leq 9\alpha \|\Delta\|_F^2 \gamma \left(1 + \frac{\|\Sigma\|}{\alpha} \right)^{1/2} \\ & \leq \frac{\lambda_r(\Sigma) - \lambda_{r+1}(\Sigma)}{2} \|\Delta\|_F^2, \end{aligned} \tag{C.16}$$

where the second last inequality follows from the assumption and $\|G - \hat{G}\| \leq \|G - \hat{G}\|_F \leq \gamma \leq 1$, and the last inequality follows from equation B.19. Combining equation C.15 and equation C.16 gives

$$\text{vec}(\Delta)^\top \frac{\partial^2 \mathcal{L}_L(G)}{\partial \text{vec}(G) \partial \text{vec}(G)^\top} \text{vec}(\Delta) \geq \frac{\lambda_r(\Sigma) - \lambda_{r+1}(\Sigma)}{2} \|\Delta\|_F^2.$$

Setting $\beta_l \triangleq (\lambda_r(\Sigma) - \lambda_{r+1}(\Sigma))/2$ concludes the proof. \square

Proof of Lemma B.7. Here we derive the minimizer of \mathcal{L}'_L . Let the singular value decomposition of Σ be $\Sigma = P\Lambda Q^\top$, where $\Lambda \in \mathbb{R}^{d_1 \times d_2}$ is a diagonal matrix and $P = (p_1, \dots, p_{d_1}) \in \mathbb{O}_{d_1, d_1}$ and $Q = (q_1, \dots, q_{d_2}) \in \mathbb{O}_{d_2, d_2}$ are orthogonal matrices. By setting equation C.9 to be 0, we obtain

$$G \begin{pmatrix} O & \Sigma \\ \Sigma^\top & O \end{pmatrix} = \alpha(GG^\top - I_r)G.$$

Equivalently,

$$G_1 \Sigma = \alpha(GG^\top - I_r)G_2, \tag{C.17}$$

$$G_2 \Sigma^\top = \alpha(GG^\top - I_r)G_1. \tag{C.18}$$

Multiplying Σ from the right in equation C.18, and substituting with equation C.17 gives

$$G_2 \Sigma^\top \Sigma = \alpha(GG^\top - I_r)G_1 \Sigma = \alpha(GG^\top - I_r)^2 G_2.$$

Thus the right singular vectors of G_2 is aligned with some r column vectors of Q . Given an indices set $J = \{j_1, \dots, j_r\}$, we write $\Lambda_J \triangleq \text{diag}((\Lambda)_{j_1, j_1}, \dots, (\Lambda)_{j_r, j_r})$, $P_J \triangleq (p_{j_1}, \dots, p_{j_r})$ and $Q_J \triangleq (q_{j_1}, \dots, q_{j_r})$. We decompose G_2 by SVD as $G_2 = V_2 C_2 U_2^\top$, where $U_2 = Q_I$ for some $I = (i_1, \dots, i_r) \subset [d_1]$ and $C_2 \in \mathbb{R}^{r \times r}$ is a diagonal matrix, and $V_2 \in \mathbb{O}_{r, r}$. Similarly, we decompose G_1 as $G_1 = V_1 C_1 U_1^\top$, where $U_1 = P_{I'}$ for some $I' = (i'_1, \dots, i'_r) \subset [d_2]$, $C_1 \in \mathbb{R}^{r \times r}$ is a diagonal matrix, and $V_1 \in \mathbb{O}_{r, r}$.

From equation C.17, we obtain

$$V_1 C_1 \Lambda_{I'} Q_{I'}^\top = \alpha (G G^\top - I_r) V_2 C_2 Q_I^\top.$$

Thus $Q_{I'} = Q_I H_Q$ for some $H_Q \in \mathbb{O}_{r,r}$. Without loss of generality, we set $I = I'$.

Since the term $-\text{tr}(G_1 \hat{\Sigma} G_2^\top) = -\text{tr}(V_1 C_1 \Lambda_I C_2 V_2^\top)$ in the loss function is minimized when $V_1 = V_2$, whereas the penalty term $\Pi(G_1, G_2)$ is invariant under the change of V_1 and V_2 , we obtain $V_1 = V_2$. In summary, from equation C.17 and equation C.18, we have

$$\begin{aligned} V_1 C_1 \Lambda_I Q_I^\top &= \alpha V_1 (C_1^2 + C_2^2 - I_r) C_2 Q_I^\top, \\ V_1 C_2 \Lambda_I P_I^\top &= \alpha V_1 (C_1^2 + C_2^2 - I_r) C_1 P_I^\top. \end{aligned}$$

Thus

$$C_1 \Lambda_I = \alpha (C_1^2 + C_2^2 - I_r) C_2, \quad C_2 \Lambda_I = \alpha (C_1^2 + C_2^2 - I_r) C_1. \quad (\text{C.19})$$

Fix any $j \in [r]$. Suppose that j -th entry of C_1 is 0. Then, from equation C.19, j -th entry of C_2 must be 0. Now the loss function can be written as

$$\mathcal{L}_L = -\text{tr}(C_1 \Lambda_I C_2) + \frac{\alpha}{4} \|C_1^2 + C_2^2 - I_r\|_F^2.$$

Note that we can make the loss smaller by slightly increasing j -th diagonal entry of C_1 and C_2 . This implies that j -th diagonal entry of C_1 and C_2 cannot be 0 when G_1 and G_2 are the solution to the minimization of the loss $\mathcal{L}_L(G)$. Since j is arbitrary, we can show that $C_1 = C_2 = (1/\sqrt{2})(I_r + (1/\alpha)\Lambda_I)^{1/2}$.

Next we show $I = [r]$. To see this, note that

$$\begin{aligned} \mathcal{L}_L &= -\frac{1}{2} \text{tr} \left(\left(I_r + \frac{1}{\alpha} \Lambda_I \right)^{1/2} \Lambda_I \left(I_r + \frac{1}{\alpha} \Lambda_I \right)^{1/2} \right) + \frac{\alpha}{4} \text{tr}((C_1^2 + C_2^2 - I_r)^2) \\ &= -\frac{1}{2} \sum_{i \in I} \left(\lambda_i + \frac{\lambda_i^2}{\alpha} \right) + \frac{1}{4\alpha} \sum_{i \in I} \lambda_i^2 \\ &= -\frac{1}{2} \sum_{i \in I} \left(\lambda_i + \frac{\lambda_i^2}{2\alpha} \right), \end{aligned}$$

which is minimized if and only if $I = [r]$ due to the assumption $\lambda_r(\Sigma) > \lambda_{r+1}(\Sigma)$. Finally, \hat{G} is given by

$$\hat{G}_1 = \frac{1}{\sqrt{2}} V \left(I_r + \frac{1}{\alpha} \Lambda_{[r]} \right)^{1/2} P_{[r]}^\top, \quad \hat{G}_2 = \frac{1}{\sqrt{2}} V \left(I_r + \frac{1}{\alpha} \Lambda_{[r]} \right)^{1/2} Q_{[r]}^\top, \quad (\text{C.20})$$

where $V \in \mathbb{O}_{r,r}$ is any orthogonal matrix. \square

D Auxiliary Results

Here we define Orlicz norm of a random variable X as $\|X\|_{\psi_2} \triangleq \inf\{c > 0 : \mathbb{E}[e^{X^2/c^2}] \leq 2\}$.

Assumption D.1. Let X and \tilde{X} be mean zero random vectors taking values in \mathbb{R}^{d_1} and \mathbb{R}^{d_2} , respectively. Assume that there exists some constants $C_1, C_2 > 0$ satisfying that $\mathbb{E}[(u^\top X)^2] \geq C_1 \|u^\top X\|_{\psi_2}^2$ holds for any $u \in \mathbb{R}^{d_1}$, and that $\mathbb{E}[(v^\top \tilde{X})^2] \geq C_2 \|v^\top \tilde{X}\|_{\psi_2}^2$ holds for any $v \in \mathbb{R}^{d_2}$.

We borrow the proposition from Nakada et al. (2023) for bounding the distance between sample cross-covariance matrix and population cross-covariance matrix.

Lemma D.1 (Proposition 9.1 from Nakada et al. (2023)). *Suppose that Assumption D.1 holds. Let $(X_1, \tilde{X}_1), \dots, (X_n, \tilde{X}_n)$ be independent copies of (X, \tilde{X}) . Let $\hat{\Sigma}_{X, \tilde{X}} \triangleq (1/n) \sum_{i=1}^n X_i \tilde{X}_i^\top$. Then, there exists some constant $C = C(C_1, C_2) > 0$ such that with probability at least $1 - e^{-t}$,*

$$\begin{aligned} & \|\hat{\Sigma}_{X, \tilde{X}} - \mathbb{E}[\hat{\Sigma}_{X, \tilde{X}}]\| \\ & \leq C \left[(\text{tr}(\Sigma_{\tilde{X}}) \|\Sigma_X\| \vee \text{tr}(\Sigma_X) \|\Sigma_{\tilde{X}}\|)^{1/2} \sqrt{\frac{t + \log(d_1 + d_2)}{n}} \vee (\text{tr}(\Sigma_X) \text{tr}(\Sigma_{\tilde{X}}))^{1/2} \frac{t + \log(d_1 + d_2)}{n} \right] \end{aligned}$$

holds for all $t > 0$.

Lemma D.2 (Corollary 2.5 from Bardenet and Maillard (2015)). *Let $X_1, \dots, X_n \in \mathbb{R}$ be fixed numbers. Let $\mathcal{B} \subset [n]$ be a random batch of size b from $[n]$ without replacement. Then,*

$$\left| \frac{1}{b} \sum_{i \in \mathcal{B}} X_i - \frac{1}{n} \sum_{i \in [n]} X_i \right| \lesssim \max_{i \in [n]} |X_i| \sqrt{\frac{(1 - b/n) \log(1/\gamma)}{b}}$$

holds with probability $1 - \gamma$.

Lemma D.3 (Modification of Lemma C.1 from Nakada et al. (2023)). *Suppose Assumptions B.4 and B.3 hold. Then, the following inequalities hold with probability $1 - O((n + d)^{-1})$:*

$$\begin{aligned} \max_{i \in [n]} \|x_i\| & \leq C_1 \|\Sigma_z\|^{1/2} \sqrt{(r + s_1^{-2} r_e(\Sigma_\xi)) \log(n + d)}, \\ \max_{i \in [n]} \|\tilde{x}_i\| & \leq C_2 \|\Sigma_{\tilde{z}}\|^{1/2} \sqrt{(r + s_2^{-2} r_e(\Sigma_{\tilde{\xi}})) \log(n + d)}, \end{aligned}$$

where $C'_1 = C'_1(\sigma, s_1)$, $C'_2 = C'_2(\sigma, s_2)$ are some constants.